# MANUFACTURING, MECHANICAL BEHAVIOR AND FAILURE ANALYSIS OF ULTRASONIC WELDED CARBON FIBER REINFORCED THERMOPLASTIC COMPOSITES

A Thesis

by

Umut ÖZKAN

Submitted to the

Graduate School of Sciences and Engineering
In Partial Fulfillment of the Requirements for
the Degree of

Master of Science

in the
Department of Mechanical Engineering

Özyeğin University
August 2020

**MANUFACTURING, MECHANICAL BEHAVIOR AND FAILURE ANALYSIS OF ULTRASONIC WELDED CARBON FIBER REINFORCED THERMOPLASTIC COMPOSITES**

Approved by:

Assoc. Prof. Dr. Güney Güven YAPICI,
Advisor,
Department of Mechanical Engineering
Head of Department
*Özyeğin University*

Assist. Prof. Dr. Görkem YILMAZ,
Department of Industrial Engineering
*Özyeğin University*

Assist. Prof. Dr. Mehmet İPEKOĞLU,
Department of Mechanical Engineering
*Turkish-German University*

Date approved: 25 August 2020

*To My Family…*

# ABSTRACT

The requirement for utilizing high-performance thermoplastic composites (TPC) has risen in the last years due to their excellent mechanical properties. Although improving mechanical characteristics of TPC is a promising development for future engineering applications, great attention has to be given on determining appropriate fabrication and joining techniques due to limitations in manufacturing technology. On the other hand, despite several research works have been conducted investigating the mechanical properties of various short carbon fiber reinforced (SCFR) TPC, the lack of knowledge about the effects of processing parameters of compression molding (CM) and ultrasonic welding (USW) on the mechanical performance of TPC was the motivation of this thesis. Accordingly, this thesis comprises a two-stage experimental approach evaluating the influences of process parameters of CM and USW on the mechanical and microstructural properties of SCFR-ABS composite under different types of loadings.

According to the mechanical tests, the tensile response of molded samples was found to be highly dependent on carbon fiber content and molding temperature, whereas impact properties were mostly affected by molding pressure. With input from the first stage, molded samples were ultrasonically welded in lap configuration to reveal the joint strength under shear. Up to 7.67 MPa lap shear strength (LSS) is achieved by experiments where welding pressure and duration were seen to have the most significance. On the other hand, energy dissipation during welding was also considered as high levels resulted in structural degradation. The mechanical responses of molded and welded samples were discussed in light of detailed fracture analysis considering the fiber-matrix interface.

# ÖZET

Yüksek performans termoplastik kompozitlerin (TK) kullanım ihtiyacı, mükemmel mekanik özellikleri nedeniyle son yıllarda artmıştır. TK mekanik özelliklerinin iyileştirilmesi gelecekteki mühendislik uygulamaları için umut verici olsa da, üretim teknolojisindeki sınırlamalar nedeniyle uygun imalat ve birleştirme tekniklerinin belirlenmesine büyük önem verilmelidir. Öte yandan, literatürde çeşitli kısa karbon elyaf takviyeli TK mekanik özelliklerinin incelenmesi ile ilgili bir çok araştırma olmasına rağmen, sıkıştırma kalıplama (SK) ve ultrasonik kaynak (UK) yöntemlerinin proses parametrelerinin malzemenin mekanik performansı üzerindeki etkileri hakkında bilgi eksikliği, bu tezin motivasyonu olmuştur. Buna göre, bu tez, SK ve UK işlem parametrelerinin kısa karbon elyaf takviyeli ABS kompozit malzemesinin farklı yük tipleri altında mekanik ve mikroyapısal özellikleri üzerindeki etkilerini değerlendiren iki aşamalı deneysel bir yaklaşım içermektedir.

Mekanik testlere göre, kalıplanmış numunelerin çekme yönündeki tepkisi büyük ölçüde karbon elyaf içeriğine ve kalıplama sıcaklığına bağlıdır, darbe dayanım özelliği daha çok kalıplama basıncından etkilenmiştir. İlk aşamadan elde edilen girdi ile kalıplanmış numuneler kayma kuvveti altında kesme mukavemetini ortaya çıkarmak için üst üste bindirilerek ultrasonik kaynaklanmıştır. Deneyler sonucunda en yüksek 7.67MPa kesme mukavemet değerine ulaşılmıştır, ayrıca kaynak basıncı ile zamanının bu değeri etkileyen en önemli parametreler olduğu görülmüştür. Ek olarak, yüksek seviyelerdeki kaynak enerjisi kompozitte yapısal bozulmaya yol açtığı düşünülmektedir. Kalıplanmış ve kaynaklanmış numunelerin mekanik tepkisi, fiber-matris arayüzü dikkate alınarak kopmuş yüzeylerin analizi ışığında tartışılmıştır.

# ACKNOWLEDGEMENTS

First of all, I deeply would like to thank my supervisor, Assoc. Prof. Dr. Güney Güven YAPICI, for his endless support and providing me a great vision throughout my study. It would be impossible for me to complete my thesis without his guidance. Therefore, I would like to express my gratitude to him.

I would like to thank my jury members, Dr. Mehmet İPEKOĞLU and Dr. Görkem YILMAZ for their guidance and support.

I would like to thank my company, Vestel Household Inc., for providing me this opportunity and encouraging me to improve myself in this field.

My deep and sincere gratitude to my beloved wife, Elif Yıldızer Özkan, for her continuous love, help and support during my study.  Thank you for being my best friend. I owe you everything.

I would like to thank my mum, Nevin Poyrazoğlu, especially for her limitless support and understanding during my research. I will never forget her moral support to me.

Finally, I would like to thank Ali Hosseinzadeh Ghobadlou who is now working as a research assistant at MEMFIS group for his contributions to this research.

# TABLE OF CONTENTS

# LIST OF TABLES

# LIST OF FIGURES

# 1. INTRODUCTION

## *1.1 Background and motivation*

Researchers have been interested in developing new advanced materials and manufacturing techniques which can be used in various industries since the industrialization age. Despite rapid technological advancements, one of the main concerns has always been as fabrication of the final product with minimum energy and cost. Therefore, the popularity of using thermoplastic composites (TPC) instead of metallic components has increased due to high potential for satisfying these conditions for the last decades.

Reinforcements have been used to improve the mechanical properties of the TPCs. Among them, carbon fiber has been the most promising reinforcement for its potential of weight reduction while exhibiting high tensile strength and modulus especially important for the aerospace and automotive industry due to strict carbon footprint regulations [1,2]. Moreover, compression molding (CM) and injection molding (IM) are the most common techniques for the manufacturing of discontinuous type of carbon fiber reinforced TPC systems and these methods give the possibility of creating complex design geometries with low-cost mass production [3,4]. However, the orientation of randomly distributed short carbon fibers in the polymer matrix is strongly dependent on the flow direction of molten composite and anisotropic mechanical properties have been observed. Therefore, investigation of the experimental parameters has been a key for understanding the mechanical behavior of short carbon fiber reinforced (SCFR) TPCs [5].

Although enhancing the mechanical performance of SCFR TPCs is crucial for future engineering applications, emphasis has to be given on the determination of suitable joining techniques due to limitations in manufacturing of complex and large structures [6]. USW is an attractive and low-cost joining method with a potential for mass production, short process durations and energy-saving characteristics [7]. High-frequency and low amplitude vibrations are exerted on the upper surface of an adherends via sonotrode during the welding process to create interfacial or viscoelastic friction [8,9]. USW mainly takes place in two phases as vibration and solidification. Vibration phase is affected by the welding force, welding duration and amplitude of vibration whereas the solidification phase is influenced by the solidification force and solidification time [10].

To sum up, the motivation of this thesis originates from the absence of a study about investigating the effects of processing parameters on the mechanical and microstructural characteristics of compression molded and ultrasonic welded SCFR-ABS composites with varying fiber content.

## *1.2 Objective for this research*

The main objective of the present study is to provide a comprehensive approach for identifying the optimum process parameters for achieving improved strength properties in compression molded and ultrasonic welded SCFR-ABS composite joints. The objective of this thesis is achieved through the following sub-objectives:

i. Define an experimental procedure of fabricating the test specimens comprising the design of molds according to the related test standards.

ii. Gaining more knowledge about the influences of processing parameters on the mechanical response of compression molded and ultrasonic welded SCFR-ABS in terms of tensile strength, ductility, impact energy and lap shear strength (LSS).

iii. Achieving the maximum LSS with minimum welding energy.

iv. Comparing the trends of mechanical behavior with the microstructure of composite in different conditions and obtaining the main fracture mechanisms from the analysis.

## *1.3 Thesis structure*

This thesis is divided into six chapters covering all sub-objectives mentioned before. In chapter 2, a literature review was done to fully represent the background of polymers, reinforcement systems, fabrication methods of discontinuous type of fiber-reinforced polymers and joining techniques of them. In chapter 3, the design of an efficient experimental method was introduced including manufacturing and testing of specimens. In chapter 4, the data obtained from chapter 3 was discussed with the perspective of influences of processing parameters on the mechanical behavior of compression-molded SCFR-ABS composite supporting with microstructural images. With input from chapter 4, the effects of processing parameters on the mechanical response of ultrasonic welded SCFR-ABS including the main fracture mechanism from microstructure was discussed in chapter 5. In chapter 6, the conclusion of the thesis was presented.

# 2. LITERATURE REVIEW

## *2.1 Introduction to polymers*

Polymers have been located on an indispensable position in daily life due to extended application areas since the last century. As polymer family expanded in years, unique characteristics such as lightweight, corrosion resistance, ease of manufacturability, transparency, cost-friendly and giving flexibility in design provide a significant advantage over other materials [11]. This availability enables to increase range of industrial products eventually growing importance in engineering applications especially in automotive, aerospace and medical sector [12,13].

Although manufacturing difficulty of polymers is lower than metals, mass production of final polymer part contains several chemical and mechanical processes. Natural resources such as oil, natural gas, chemicals etc. are chemically treated and monomers which are the smallest molecules in polymer chain are created. Chemical composition of a polymer resin consists of uniting many monomers and creating polymer chains with different molecular weights called polymerization process. After this process, polymers are generally formed as granules, flakes, powder, pellets and liquids. Physical and mechanical properties of polymers are improved by adding some pigments, plasticizers, stabilizers, reinforcements, flame retardants depending on the application. These compounds are then fabricated with different manufacturing methods such as injection molding (IM), compression molding (CM), blow molding, thermoforming, rotational molding [14]. Generally, polymers are classified into three main groups based on mechanical, thermal and microstructure properties [15,16] as shown in Fig.2.1 below;

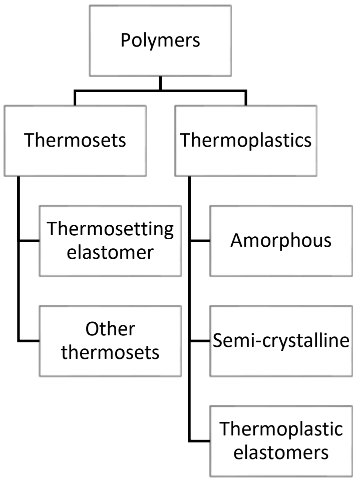


**Figure 2.1** Classification of polymers

### 2.1.1 Thermosetting polymers

Thermosets are created by a mixture of a resin and curing agent which helps to start chemical reaction under appropriate thermal conditions. This reaction is called cross-linking of monomers which also formed them a complicated network structure. However, this polymerization reaction may last from minutes to hours depending on curing system, therefore requested product can be molded during this period [17]. Mostly used thermosets in engineering applications are shown in Table 2.1.

**Table 2.1** Properties of commonly used thermosetting polymers [17]

| Polymer | Density ($g/cm^3$) | Tensile modulus (GPa) | Tensile strength (MPa) | Elongation at failure (%) |
|---|---|---|---|---|
| Polyester | 1.1-1.43 | 2.1-3.45 | 34.5-103.5 | 1-5 |
| Vinylester | 1.12-1.32 | 3-3.5 | 73-81 | 3.5-5.5 |
| Epoxy | 1.2-1.3 | 2.75-4.10 | 55-130 | - |

Despite engineering thermosets exhibit higher mechanical and thermal properties such as low creep resistance and higher durability to thermomechanical loads than thermoplastics, the biggest disadvantage is not having a recycle process due to curing [18].

### 2.1.2 Thermoplastic polymers

Thermoplastics differ from thermosets according to the input agent which is the key element of manufacturing process of a plastic part. Unlike thermosets, thermoplastics melt while heat is applied, change their phase (heat-softened phase or liquid phase) during processing and do not need any curing. Therefore, the biggest advantage of using thermoplastics is having ability to be recycled over and over with the application of heat. Moreover, thermoplastics exhibit higher performance in some mechanical properties such as higher ductility and impact resistance values comparing to thermosets. In addition, joining techniques such as vibration welding, resistance welding and ultrasonic welding (USW) can be effectively used for complex thermoplastic parts. Manufacturing process time is another advantage of thermoplastics because they do not need any chemical reaction (curing) which extends the time [17].

On the other hand, a special form of synthetic polymers is classified as engineering thermoplastics which demonstrate superior performance in mechanical properties such as corrosion resistance, transparency, lightness, ductiliy, tensile modulus and ease of production. Therefore, structural durability in long-life from disturbances like mechanical stress, impact, flexure, vibration, friction and temperature differences is much higher which makes them eligible alternative to metals [19]. As it is shown below, Table 2.2 listed popularly used engineering thermoplastics with their own polymer structure and mechanical properties.

**Table 2.2** Properties of commonly used engineering thermoplastics [20]

| Polymer Name | Polymer structure | Mechanical properties |
|---|---|---|
| Acrylonitrile butadiene styrene (ABS) | Amorphous | Good strength, stiffness and toughness. |
| Polypropylene (PP) | Semi-crystalline | Good chemical resistance, relatively low-cost. |
| Polyethylene (PE) | Semi-crystalline | Good wear resistance, excellent chemical resistance. |
| Polycarbonate (PC) | Amorphous | Stiff, strong and good ductility. |
| Polyamide (PA) | Semi-crystalline | Good tensile strength and resistance to wear. |
| Polymethylmethacrylate (PMMA) | Amorphous | High transparency, low-cost. |
| Polyvinylchloride (PVC) | Amorphous | Low-cost, easy to process. |
| Polyurethane (PU) | Amorphous | Good abrasion resistance, retention in low temperatures |
| Polyetherimide (PEI) | Amorphous | Long-term heat resistance, dimensional stability. |
| Polyetheretherketone (PEEK) | Semi-crystalline | High strength and toughness, high chemical resistance. |

## *2.2 Fiber reinforcements used in thermoplastic composites*

Emerging need to superior mechanical or chemical properties in some engineering applications lead creation of the composite materials which consist of two or more chemically bonded different materials whose content is generally defined as matrix and reinforcements [21]. The composite is called thermoplastic composite (TPC) if the matrix of the composite is a thermoplastic material, however reinforcements can vary as particles, whiskers or fibers. Particles are not preferred due to misorientation disadvantage and limited capacity of mechanical improvement. On the other hand, the challenge of uniform dispersion of whiskers in polymer matrix is the biggest concern as load transfer from matrix to reinforcement is smaller when external load is exerted. However, fibers are mostly used in advanced engineering applications due to their microstructure advantage, capability of lightweight design, higher stiffness and strength values [22]. Important mechanical and physical properties of commonly used fibers are demonstrated in Table 2.3.

The first common fiber type is glass fibers whose raw material is bulk glass. As can be seen from Table 2.3, there are several types of glass fibers which are manufactured according to desired mechanical, thermal or electrical properties. Enhanced strength and good chemical resistance are mostly provided with E-glass fibers. On the other hand, S-glass fibers have higher tensile strength compared to E-glass fibers but have less application area due to high cost. Different types of glass fibers are used in wide range of application areas from military and aerospace high-standard level to daily-life low-standard plastics [21,22,23].

**Table 2.3** Properties of commonly used fibers [22]

| Fiber type | Tensile strength MPa | Tensile modulus GPa | Elongation at failure % | Density ($g/cm^3$) | Fiber diameter μm |
|---|---|---|---|---|---|
| E-glass | 3450 | 68.95 | 4.7 | 2.58 | 5-20 |
| S-glass | 4480 | 86.9 | 5.6 | 2.48 | 5-10 |
| Kevlar 29 | 3620 | 82.7 | 4.0 | 1.44 | 12 |
| Kevlar 49 | 3790 | 131 | 2.8 | 1.44 | 12 |
| Kevlar 149 | 3450 | 186.2 | 2.0 | 1.47 | 12 |
| SM PAN-based carbon | 3450-4830 | 220-240 | 1.5-2.2 | 1.80 | 6-8 |
| IM PAN-based carbon | 4140-6200 | 275-296 | 1.3-2.0 | 1.80 | 5-6 |
| HM PAN-based carbon | 4140-5515 | 345-448 | 0.7-1.0 | 1.90 | 5-8 |
| LM Pitch-based carbon | 1380-3100 | 170-240 | 0.9 | 1.9 | 11 |
| HM Pitch-based carbon | 1900-2760 | 380-620 | 0.5 | 2.0 | 11 |
| UHM Pitch-based carbon | 2410 | 690-965 | 0.3 | 2.2 | 10 |

SM: Standard modulus, IM: Intermediate modulus, HM: High modulus, LM: Low modulus, UHM: Ultra-High modulus

The second popular type is aramid fibers which are also known as polymeric fibers. The main characteristics of aramid fiber are having high tensile strength to weight ratio and high modulus to weight ratio due to its low density, therefore aramid fiber reinforced composites are preferred in aerospace and body armors for military applications. However, having low compressive strength, low creep resistance, easiness to absorb moisture and sensitivity to UV light are the disadvantages of this fiber type [21,24].

The third and most promising type is carbon fibers whose trend of application in fiber reinforcement systems rises exponentially in the past decades. The reason of this growth originates from superior mechanical, thermal and electrical characteristic of carbon fibers such as excellent strength and stiffness, fatigue resistance, corrosion resistance, low thermal expansion and electrical conductivity [19,23]. According to reasons listed above, carbon fiber reinforced polymer (CFRP) systems have been considered as high performance materials and used as replacement with metallic components. Furthermore, it is demonstrated from the Table 2.3 that there are several manufacturing methods of carbon fibers from different precursors showing various mechanical property values, the most popular ones are PAN (polyacrylontrile) and pitch based carbon fibers [24]. As efficiency of these production methods get higher or new methods are developed for cheap and reliable solution, the usage of CFRP systems will be increased rapidly.

### 2.2.1 Continuous type of fiber-reinforcements

Matrix of the polymer composite systems can be either thermoplastic or thermoset resin, however fiber reinforcement of the system vary with type of fiber (glass, carbon etc.), geometry of fiber (continuous or discontinuous) and structure (random or oriented). Therefore, arrangement of the fibers is critical for the product because stiffness and strength of the composite are directly related with fiber orientation. Furthermore, increasing aligned fiber content in load direction proportionally increases the stiffness and strength of the composite along load direction.

In order to manufacture continuous type of fiber-reinforced thermoplastic composites, layers of unidirectional yarns are aligned along the load direction and impregnated with the resin with a specific fiber content and yarn distribution. Group of these layers is defined as laminates. This process is called prepreging and this unidirectional sheets give user to flexibility of stacking sequence of composite. After then, the curing process of the composite starts with the help of heat and pressure which are the final steps of manufacturing [23].

### 2.2.2 Discontinuous type of fiber-reinforcements

Discontinuous or short fiber reinforcement systems have been frequently used in many engineering areas due to their cost-friendly structure, enhanced mechanical properties and ease of production. Despite advantages mentioned above, higher strength and stiffness value of these systems can not reach continuous type of fiber reinforcement systems because short fibers which are compounded with the matrix are randomly oriented and anisotropic mechanical properties are observed in the composite. However, continuous reinforcement systems have more complex, expensive and low-volume manufacturing processes [22]. Based on these distinctions, fiber reinforcement system should be carefully chosen by related application or requirement. Even though there are lots of fiber types available, E-glass fibers are the most popular one used in short fiber reinforced systems as they are cost-friendly relative to other fiber types, and they have a compatibility with the most of the polymers improving mechanical and physical properties of them [22].

CM, IM and additive manufacturing (AM) technologies are generally used for high-volume production of these kind of composites. However, decrease of fiber length and misorientation of short fibers during these production methods are the biggest concerns which directly affect the mechanical properties of the composite [3,4,5].

### 2.2.3 Carbon fiber as a reinforcement

Recently, carbon fibers have become popular and classified as high performance fibers due to their excellent mechanical properties with good thermal stability and low density. These fibers are generally manufactured from a raw material called ‘precursor’. Polyacrylonitrile (PAN) is the most famous precursor to produce high amount of carbon fibers as it is economical to use as a raw material [19,25]. Forming carbon fibers from PAN requires a series of processes following as; polymerization of PAN, spinning of fibers, thermal stabilization, carbonization, graphitization, and surface treatment. After fibers are chemically, thermally and mechanically stable, spinning machine helps fibers to be twisted into yarns of different sizes so called ‘continuous carbon fibers’ [25]. Furthermore, unidirectional tape of carbon fibers can be milled to form chopped or short fibers having a length ranging from 3.2 to 50mm. Short carbon fibers are mostly suitable for reinforcing thermoplastic resins to improve mechanical properties [22].

### 2.2.4 Applications of thermoplastic composites

Applications based on both continuous and discontinuous type of fiber reinforcements have grown up for the last decades especially for aerospace, automotive and marine manufacturers. In fact, some of the aerospace manufacturers have started replacing metallic components with TPC such as J-nose of an aircraft as it was studied that manufacturing of this component with carbon fiber reinforced PPS not only provides load-bearing characteristic but also has acceptable cost range [26]. Furthermore, short fiber reinforced TPC parts are used in interiors, secondary and semi-structural parts such as press-formed ribs, press-formed brackets, clips and cleats for various aerospace manufacturers [27]. For automotive industry, it was reported that continuous carbon fiber reinforcement with fast-curing epoxy resin has already been used in automotive structural parts via high-pressure resin transfer molding to reduce weight of the car and increase fuel efficiency. On the other hand, the same reinforcement with a thermoplastic resin was first used to produce fuel cell stack tray of a car [2]. In contrary, short carbon fiber reinforced thermoplastic parts are mostly preferred in non-structural parts such as intake manifolds, clutch pedals and accelerator pedals [28].

## *2.3 High-volume manufacturing methods of short fiber reinforced thermoplastic composites*

It has been discussed so far that mechanical properties of short fiber reinforced thermoplastic composites (SFR-TPC) are mainly influenced by type, geometry and structure of the reinforcing fibers. Despite this fact, variabilities in manufacturing processes of high-volume production have also been an effective parameter for the quality and performance of final product. The stability in fiber orientation, the homogeneity of resin matrix and fibers, adhesion between matrix and fibers after manufacturing, process temperature, process pressure and some others depending on the production method are the key parameters effecting final properties of product as important as reinforcing systems [29].

SFRC can be manufactured by conventional compression molding (CM) [30] or injection molding (IM) [31] processes or innovative additive manufacturing (AM) technique especially having a tendency with fused deposition modeling [32]. Each production method has its own advantages and disadvantages while manufacturing of SFR-TPC systems depending on the application.

### 2.3.1 Compression molding

CM has been a traditional but popular manufacturing method to form an unreinforced or reinforced polymer resin inside of the mold with the help of pressure and temperature since 1950s especially in automotive industry [29]. Generally, fabrication of a thermosetting plastic via CM is quite simple as the system has the related mold of final product which is heated according to thermoset resin before the process. The pre-heated thermoset resin whose temperature is almost at the curing stage temperature is then poured into the mold cavity. After the mold is closed, the required pressure is exerted with the hydraulic press to form liquid polymer to become the shape of the mold. Unlike thermosetting plastics, thermoplastics need one extra process which is cooling of the mold before ejection of the part [33,34]. The schematic view of CM technique is illustrated in Figure 2.2 below.

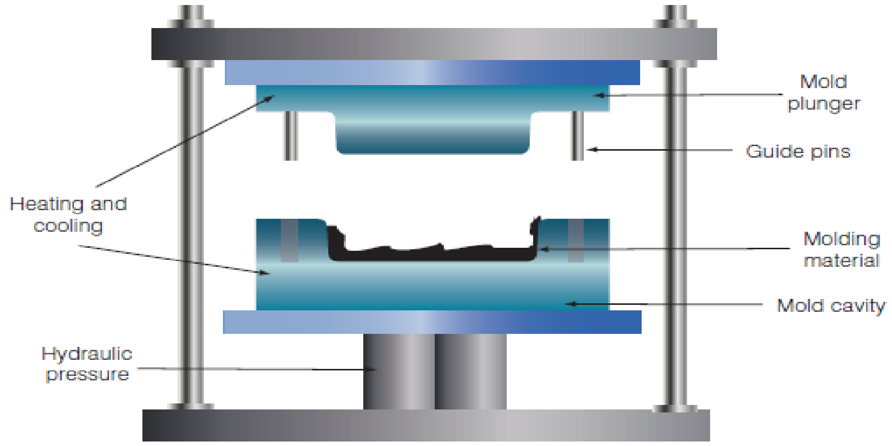


**Figure 2.2** Schematic view of CM process [35]

For the SFR-TPC systems, the mixture of short fibers and thermoplastic polymer is compounded with single or twin screw extruder according to desired mixing ratios before molding procedure. The compound is then loaded to pre-heated mold cavity before it is cooled at ambient temperature [5]. This feeding is done continuously to satisfy a consistent high-volume manufacturing of SFR-TPC systems.

On the other hand, many studies were conducted by conventional CM technique in the literature about SFR-TPC systems, especially in short glass or carbon fiber reinforcement, investigating various mechanical properties and their enhancements. Tekinalp et al. [36] had a research which demonstrates a significant increase in tensile properties of short carbon fiber reinforced (SCFR) ABS composite compared to unreinforced ABS. Moreover, microstructure analysis about fiber orientation and void formation of SCFR-ABS composite and unreinforced ABS was related with mechanical performance. Song et al. [5] reported a novel computer-aided engineering (CAE) method to predict warpage behavior of SCFR-PA6 composite fabricated with CM technique. For a deeper computational research, Song et al. [37] investigated the impacts of initial fiber orientation of SFR-TPC systems on the final fiber orientation with CM manufacturing method and developed an algorithm to predict fiber orientation in each axis after fabrication. It was advised to take into consideration of this algorithm in CM simulations to get better results.

### 2.3.2 Injection molding

IM has been a vital polymer processing method which enables to manufacture complex-designed plastic parts with high-volume production capacity and superior precision. Similar to CM, polymer resin is formed into the mold with the help of heat and pressure [34,38]. However, IM machines have higher clamp pressure capacity than CM machines which counts as an advantage for precise production. Moreover, polymer resin is melted with friction through a reciprocative screw extruder which provides IM to be a recyclable polymer processing technique.

SFR-TPC systems can be injection-molded, however polymer and reinforcement need to be mixed homogenously and extruded as granular form before injection process. A typical IM machine consists of a hydraulic cylinder and clamp for controlling pressure of the system, a hopper for resin feeding, an injection unit having reciprocating screw for heating and injecting of polymer, mold having cavity and core side with cooling channels and an electronic control unit which possess settings of injection parameters. A screw-type IM machine is demonstrated in Figure 2.3 below.

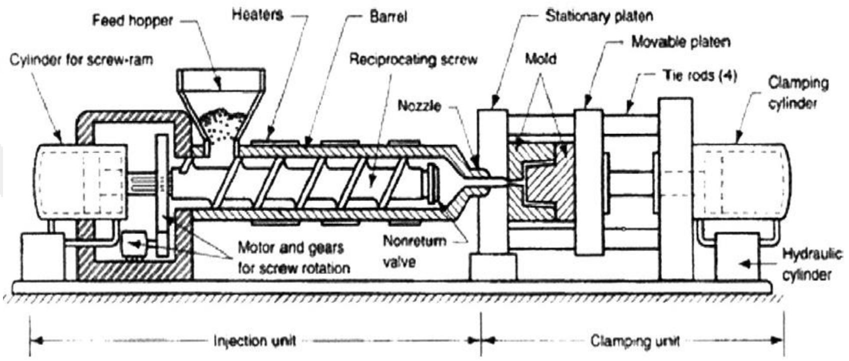


**Figure 2.3** Schematic view of screw-type injection molding (IM) machine [39]

IM process starts with the feeding of granular-formed polymer resin into the hopper. Then, the outer circumference of screw is filled with the polymer. This feeding is carried on continuously for stability of process. During this operation, screw is reciprocating along mold direction with the polymer which starts to melt with high shear forces due to movement of screw. The preheated barrel wall also helps accelerating melting process of polymer with heat conduction. After a while, the molten polymer is piled up in front of the screw whose position is set with the hydraulic pressure system according to required shot volume.

This specific shot is then injected to the mold cavity through runner and gate systems when the screw moves along mold direction and applies high pressure which is called injection pressure. The molten polymer is forced to form the shape of cavity with a specific period of time called packing pressure. Furthermore, temperature of cavity and core side of the mold needs to be under control with cooling process depending on microstructure of polymer. During this process, the polymer is cooled down with circulating water and shrinked rapidly. After cooling stage, desired plastic part is ejected from the mold with the help of ejector pins [29,33,34,38,39]. IM process including all stages are illustrated in Figure 2.4 as below.

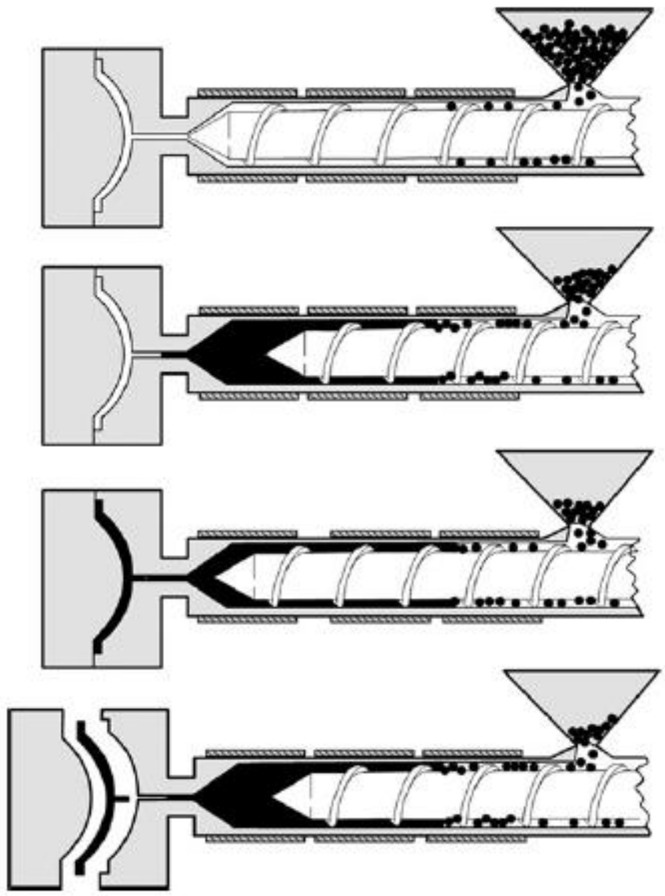

**Figure 2.4** Schematic view of screw-type injection molding (IM) process [29]

In literature, several studies were reported about investigating different mechanical properties and microstructural analysis of SFR-TPC systems with IM manufacturing technique due to its preferability against CM method. The tensile properties of injection-molded short glass fiber (SGF) and short carbon fiber (SCF) reinforced PP composites were depended on fiber volume fraction, mean fiber length and their mutual effects. In the same time, two factors were related with each other as increase of fiber volume fraction in the composite lead to decrease in fiber length [3]. Furthermore, the fracture toughness of SGF and SCF reinforced PP composites were investigated in terms of microstructure, fiber volume fraction and combined effects. It was revealed that fracture toughness was enhanced up to a threshold value of fiber volume fraction but overpassing this value caused a decrease [40]. In another research with a novel thermoplastic matrix, it was found that elastic modulus and thermal conductivity of SCFR polyketone (PK) composite were significantly improved with increasing carbon fiber content [41]. Moreover, Li et al. [42] studied the effects of adding up $HNO_3$-treated SCFs and PA6 with different mixing ratios to ABS matrix on tensile properties. PA6 inclusion and surface treatment to SCFs was an effective improvement on tensile modulus and tensile strength due to increased interfacial adhesion between matrix and reinforcement. Furthermore, Kuram et al. [43] focused on analyzing the effects of injection parameters and the amount of recycle of SGF reinforced PA6 composite with Taguchi experimental design method. It was observed that mechanical properties were mostly affected by the number of recycling. Karsli et al. [44] investigated that tensile strength, modulus and hardness of SCFR-PA6 composite improved with SCF involvement but tensile at break was negatively affected. It was concluded that optimizing extrusion and injection parameters would enhance tensile properties as fiber breakage was observed during processing. In order to prevent fiber breakage during extrusion or injection, Ozkan et al. [45] studied effects of different types of protection chemicals on tensile properties of SCFR polycarbonate (PC) composites. It was revealed that tensile modulus and strength were improved with SCF having sizing agents compared with those not having agents. In further research, effects of variance in fiber length and orientation of injection-molded

SCFR-PA6 composite with different injection rates were investigated to determine microstructure characteristics. The results demonstrated that increase in fiber content and processing rate lead a significant drop of average fiber length due to higher shear forces which directly affects mechanical properties [46]. In addition, microfailure mechanism of SGF reinforced PA6,6 composite was investigated under tensile loading with injection molding technique. It was established that microfailure of composite started with developing stress concentration points at the fiber tips and along the fiber sides which resulted in crack propagation through entire matrix [47].

### 2.3.3 Additive Manufacturing

AM has become an extremely popular and challenging method for producing reinforced polymer structures without any tool requirement compared with CM and IM techniques. Desired parts are built up through layer by layer process and AM provides a wide range of geometry possibilities and flexibility to manufacturers with low cost [48]. Another advantage is that this technology reduces scraps and increases efficiency compared with conventional manufacturing methods whose main logic is to remove material with machining [48,49].

Fused deposition modeling (FDM) is one of the most preferred AM method for printing complex parts with polymers or advanced thermoplastic composites. The main advantages of FDM are expressed as providing high dimensional accuracy of parts, simplicity, rapid processing and cost-friendly nature [50,51]. The schematic diagram of FDM is illustrated in Figure 2.5 below.

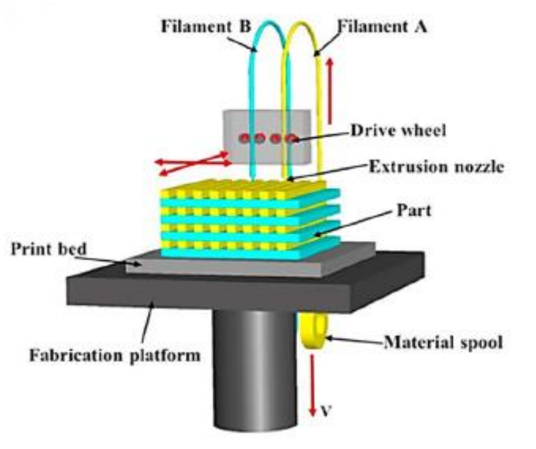


**Figure 2.5** Schematic view of FDM process [52]

As shown above, desired part is manufactured layer by layer and each layer is extruded through nozzle with an infinite filament supply. Filaments are heated up to the temperature at which polymer is reached just above its melting point and transferred to semi-liquid phase at the nozzle. After then, this new layer is deposited with the help of immediate solidification of polymer at ambient temperature on the last layer and this process is continued until manufacturing is finished [52].

Similar with other manufacturing methods, FDM of polymers has its own process parameters affecting mechanical properties and quality of final product such as layer thickness, layer orientation, raster angle and air gap. However, the difficulties of SFR-TPC systems are passed beyond these parameters mentioned above. Mechanical properties are also influenced by fiber orientation, interfacial adhesion of fiber and matrix and void formation of thermoplastic composite during FDM [52,53].

Recently, many studies about investigating the effects of printing parameters and fiber inclusion on different mechanical properties were accomplished with AM method. Ning et al. [54] studied the impacts of short carbon content fraction in weight and fiber length on the mechanical characteristics of SCFR-ABS composite. It was found that adding carbon fibers up to %7.5 into system increased tensile strength and elastic modulus, however a drop in toughness, ductility and yield strength was observed. The same result was explored by another research, however experiments also showed that thermal stability of composite is increased as carbon fiber content grows up [32]. Tekinalp et al. [36] investigated the effects of short carbon fiber content and microstructure characteristics including fiber orientation, void formation and dispersion on mechanical properties of SCFR-ABS composite via FDM. Although tensile strength increases with a rise of fiber contet, pre-mixing procedure of ABS polymer and carbon fiber is the main responsible for decreasing fiber length which directly affects tensile properties. Zhang et al. [55] focused on identifying interfacial bonding strength of virgin ABS, carbon nanotube reinforced ABS and SCFR-ABS by FDM. Increasing printing speed and layer thickness negatively affected shear strength of composites. In addition, microstructe analysis of fractured surfaces demonstrated that matrix fracture, fiber pull-out and fiber debonding from matrix are the major findings.

Furthermore, Zhang et al. [56] investigated the impacts of process parameters of FDM on the residual stress and deformation of virgin ABS, carbon nanotube reinforced ABS and SCFR-ABS. Raster angle was found to be the most influential process parameter on shrinkage and porosity level of composite. In addition, Weng et al. [57] studied mechanical properties of a novel organic modified montmorillonite (OMM) reinforced ABS nanocomposite with FDM technique. The results demonstrated that the value of tensile strength of composite was significantly rised up by 43% with adding up 5% of OMM. Some other mechanical properties such as elastic modulus, flexural strength, flexural modulus and dynamic mechanical storage modulus were also increased with involvement of OMM.

## *2.4 Joining methods for thermoplastic composites*

Nowadays, TPC structures have been widely preferred in aerospace, automotive and marine industries due to their advantages such as higher strength to weigth ratio, recyclability and resistance to mechanical loads over metallic or thermoset counterparts. However, limitations in manufacturing or assembling of large structures with TPCs have been one of the biggest obstacle so far. Therefore, joining techniques of TPCs have been located an important position in order to succeed cost-effective manufacturing [58,59].

The main joining methods are classified into three named mechanical fastening, adhesive bonding and polymer fusion bonding [58,59] as shown in Fig. 2.6 below;

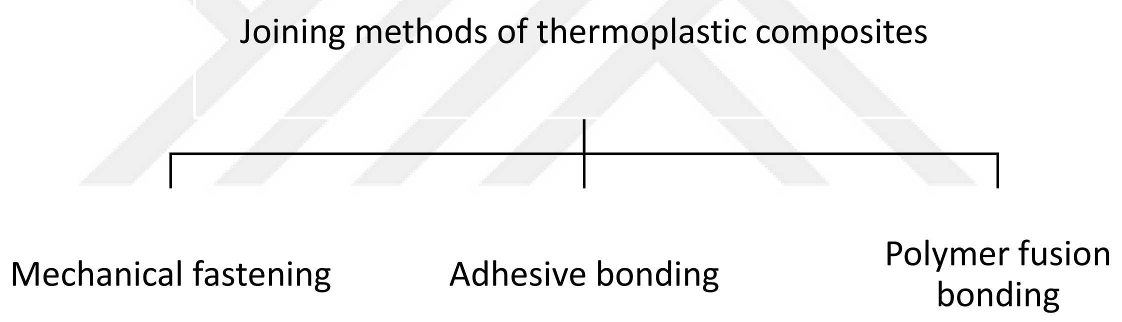


**Figure 2.6** Main groups of joining methods of TPCs [58,60]

### 2.4.1 Mechanical fastening

Mechanical fasteners such as bolts, rivets or pin-connectors have been commonly used in manufacturing of joint structures originated from TPCs due to their excellent strength capacity, ability of disassembly, no requirement of surface preparation, relatively good service temperature and durability to humidity [61]. However, one of the biggest concern of using mechanical fastener is having necessity of drilling a hole which generates local stress concentration points. Therefore, failure mechanism of mechanically fastened joints originate from these points [62]. Another disadvantage is that each mechanical fastener used in the system comes up with extra weigth, cost and low sealing capacity problems. Furthermore, drilling a hole and assemblying a fastener with undesired torque values result in cracks in thermoplastic composite structures which have sensitivity of these processes [63]. In addition, the failure characteristics of mechanically fastened joints are generally dependent on experimental data in the literature due to having different design considerations. Therefore, material, quantity and location of fastener options should be carefully selected in TPC structures for satisfying high strength joints [64].

### 2.4.2 Adhesive bonding

Instead of using mechanical fasteners, another efficient technique for joining TPCs is adhesive bonding. However, polymers are generally appeared in the nature with hydrophobic characteristic which suffers from poor surface energy. Therefore, preparation of polymer surface treatment is the most critical operation during this joining process. Otherwise, joints can fail before the load that adhesion withstands [65]. On the other hand, one of the biggest advantage of choosing adhesive bonding method over mechanical fastening is that stress is distributed uniformly through the joint and drilling is not required. Also, sealing properties of joints are improved with adhesive bonding method. However, once adhesion is completed, the process can not be reversed which means it is impossible to unassemble without damage the joint. In addition, curing period of adhesives are long which negatively affects manufacturing times in mass production [59,66].

### 2.4.3 Polymer fusion bonding

Apart from mechanical fastening and adhesive bonding, fusion bonding is the most promising joining method for TPC structures due to ability of overcome the disadvantages of other techniques mentioned in the last sections. The main idea of fusion bonding is to melt the surface of two adherend polymers with an input so that polymer chains in each surface are joined and loads can be transferred through welding area. Viscoelastic behavior is observed during the welding process as the state of the polymer on surface is viscous. Fusion bonding methods are categorized according to the input mechanism, generally named as thermal welding, friction welding and electromagnetic welding [58,60,67].

Hot-tool welding is a process which uses a hot metal plate located between two adherends in order to join parts. This method has two main operation; hot-tool is fixed between two adherends with the help of pressure in the first phase. Surfaces which are contacting with hot-tool reach the melting point and start to melt during this phase. After then, hot-tool is subtracted rapidly and two adherends are pressed until surfaces are joined with solidification of polymers [58,68]. The schematic view of this technique is demonstrated in Fig. 2.8 below;

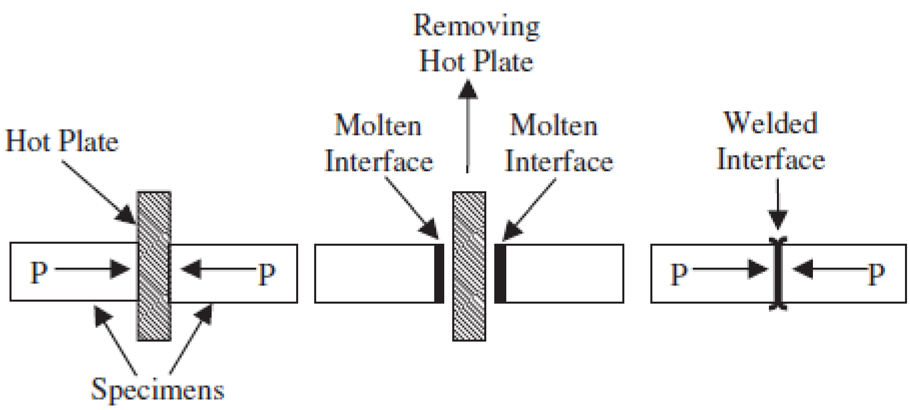


**Figure 2.7** Hot-tool welding of thermoplastic composites [58]

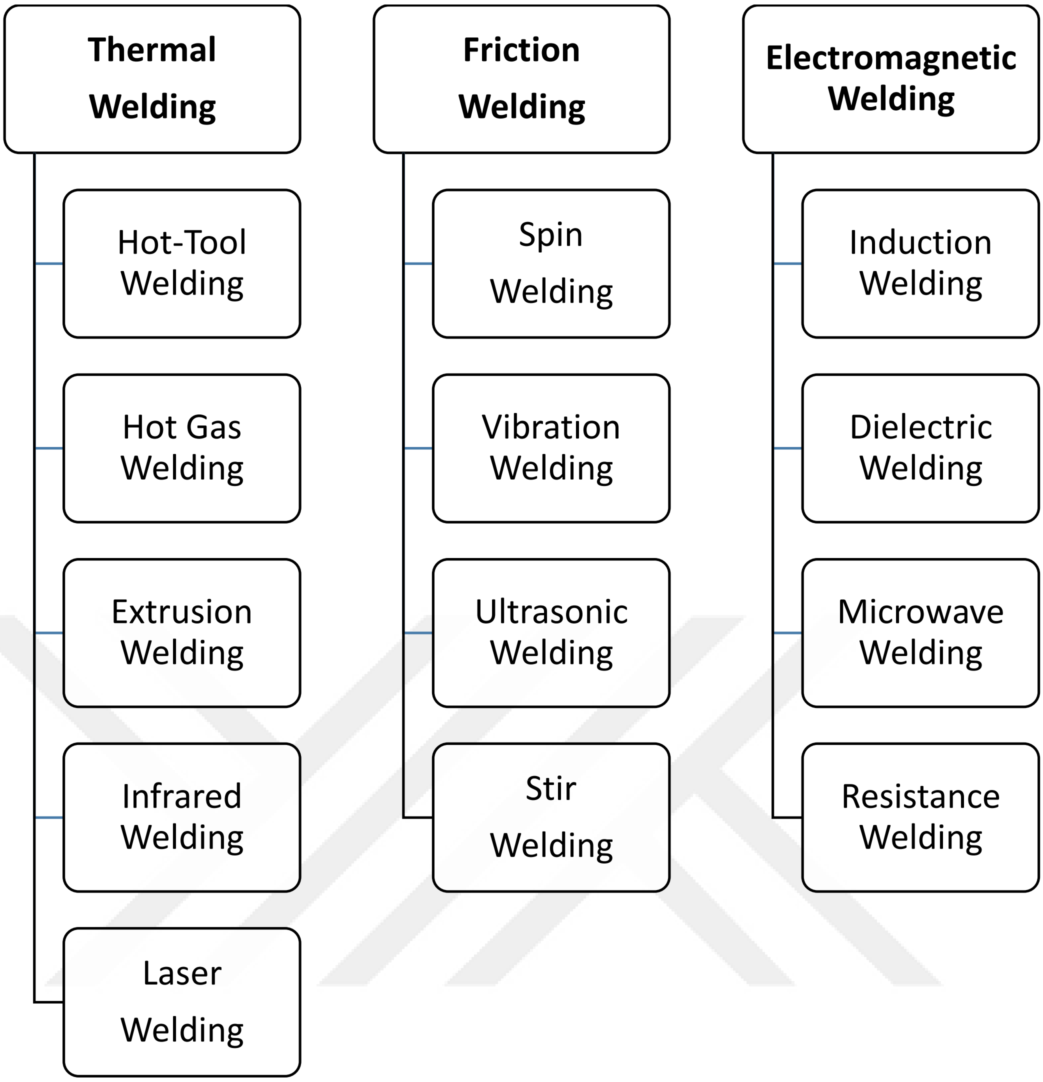


**Figure 2.8** Main groups of fusion bonding methods of TPCs [58,60,67]

Hot gas welding is another thermal welding method which uses a hot air stream as an input in order to weld thermoplastic parts. In general, gas metal welding and hot gas welding of thermoplastics share the same logic with different fillers. However, in hot gas welding, surfaces of weld groove and welding rod are heated up with hot gas until polymers are getting semi-liquid phase in order to fill the groove with pressure. Therefore, this method is usually used for repairing non-disposable plastic parts not for mass manufacturing because it is slow and operator dependent [69].

Extrusion welding technique is parallel with hot gas welding both require hot gas as an external heat input. The only difference is that filler which is already softened before welding process is extruded through the welding area continuously. Therefore, both hot gas welding and extrusion welding methods are preferred frequently in complex and large structures like big containers or vessels. However, these techniques are manually operated which make them difficult to control [58,70].

Infrared welding uses infrared radiation to melt joining surfaces of adherends without contacting and the procedure is similar with hot-tool welding. However, infrared lamps and metal plate with electrically heated are source of infrared energy to melt the polymer surface. Heating time of adherends, pressure, heat source location and change-over time are the most important factors affecting weld quality and strength [71].

In laser welding, a strong laser beam is continuously applied along the butt or lap-joint bondline configuration of adherends. During this operation, some of the polymer is burned or degraded due to laser beam interaction but there are some molten polymer layer along the path. Therefore, two layers are joined when solidification starts with the help of pressure. Laser power, scan speed, uniformity of laser beam, clamping pressure and absorption properties of the material at the bondline are the process parameters which give the biggest impact on weld quality [67,71]. Laser welding process is demonstrated in Fig 2.9 below;

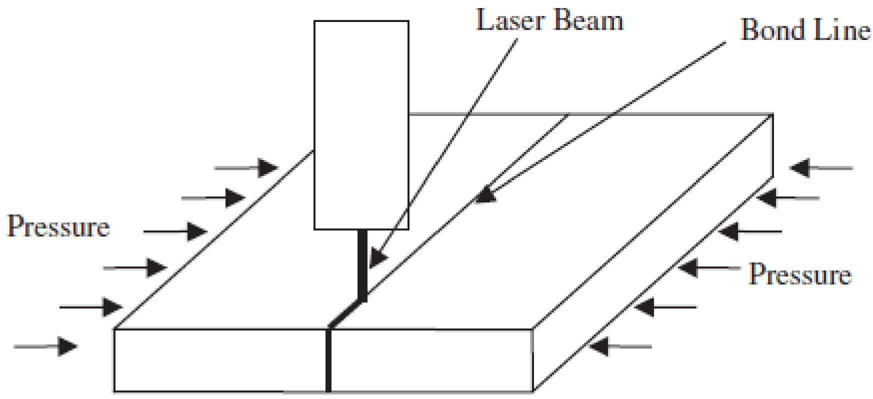


**Figure 2.9** Laser welding of thermoplastic composites [58]

Joining of TPCs with spin welding are provided with a rotational move of a part against fixed part. When sufficient friction is generated with heat and pressure, surfaces of adherends start to create a molten polymer layer which helps welding. This frictional bonding method is common in parts with having especially circular cross-section. Influential parameters vary with microstructure of polymer, angular velocity of moveable part, axial pressure, rotation time and braking time [58,71].

Vibration welding has been a popular linear frictional welding technique which uses vibrations in order to generate friction between two parts at certain pressure, frequency and amplitude. Once heat caused by frictional forces is enough to reach polymer melting point, two parts are joined and solidified together. According to this method, one part is fixed and the other one linearly moves with vibration along the welding path. This linear motion ends up with the full alignment and join of two parts with pressure. The key parameters affecting vibration welding are expressed as welding pressure, vibration amplitude, vibration time and microstructure of TPC [72].

In USW process, high frequency vibrations are converted into mechanical frictions which eventually cause heat generation at the welding area. The process seems similar to the vibration welding, however the only difference between them is that both parts are fixed in USW and a horn is used for transfer vibration with also exerting a welding pressure at the upper surface of adherend. Therefore, USW has wide range of application areas due to its rapid processing time, tendency of being automated and having high-quality welds. USW machine which contains an electric generator, converter, booster, horn and control unit is required for this process. Parts are mounted on a fixture and clamped in case there will not be any slipping of parts. The critical process parameters are welding pressure, welding duration, amplitude of vibrations, geometry of energy director and type of TPC [73].

In frictional stir welding process, joining of parts are provided with a rotational tool which is composed of two sections as shoulder and probe. The probe of this tool is plunged at the weld zone until shoulder is fixed at the top surface of parts. Then, rotational tool moves along the welding path which generates frictional heat and this work is sufficient for melting the polymer at the welding path. This rotational move also helps to accelerate the mixing of polymers which also result in solidification and so called welding of two parts [74].

A schematic illustration of this process is shown in Fig. 2.10 below;

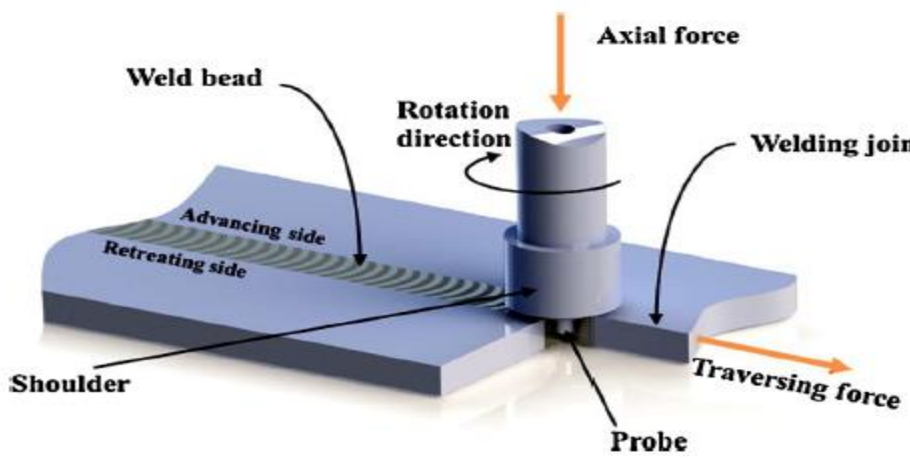


**Figure 2.10** Frictional stir welding of TPC [74]

Induction welding consists of a conductive plastic implant which is located at welding zone. The geometry of this material fits the bonding area and it is made of ferromagnetic materials. An induction coil is used to generate electromagnetic field which is captured by implant. After then, the temperature of implant rises until it starts to melt the surrounding polymer surface and provides welding of two parts. However, the conductivity of polymers is relatively low but this method is suitable for carbon fiber reinforced TPCs because carbon fibers has excellent conductivity and there is no need for extra material at the weld zone to absorb induced energy from coil. Furthermore, weld strength is fully depended on coil design and position, induction time and polymer type [71,75,76].

In dielectric welding, an intensive electromagnetic field whose frequency interval is in MHz is concentrated on the parts to be joined. This electromagnetic field is supplied with electrodes which compress the adherends at the same time. According to this technique, welding duration and strength vary with polar groups in the molecular structure of the polymer as these groups affect electromagnetic fields. Moreover, dielectric loss factor is a game-changing parameter which specifies the weld quality. Polymer generates more heat with rapidly if it has higher dielectric loss factor. Therefore, the application range of this welding method is restricted due to having lots of disadvantages compared to other types [58,71].

Microwave welding is the combination of induction and dielectric welding with higher frequency range up to GHz. Irradiation of microwaves to the polymers is not as much as effective way to rise up polymer temperature itself, therefore a conductive implant is inserted at the weld zone similar with induction welding in order to reduce polymer melting duration. In addition, this method is perfectly suitable for welding of thin sheet films. However, welding geometry is limited with simple orientations which makes this welding not to be considered for mass production [58,67,71].

In resistance welding, an electrically conductive implant which is generally metal is used between the parts to be joined. As electrical current flows through the implant, it starts to dissipate heat which cause polymer to melt at the welding zone. After solidification and welding, the heating element is remained between the parts. It is cheap, rapid and has welding capacity of big and complex structures. Therefore, this technique can be used in wide range of applications in aerospace, automotive and other fields. However, the biggest disadvantage is difficulty in heat distribution along weld line [78,79]. General principle for resistance welding is shown Fig. 2.11 below;

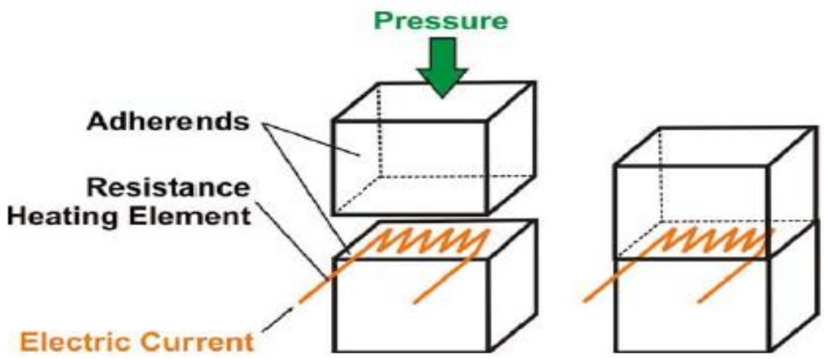


**Figure 2.11** Resistance welding of TPC [78]

## *2.5 Ultrasonic welding of thermoplastic composites*

In the last section, several joining methods are discussed in terms of advantages and disadvantages for thermoplastic composites. Among them, USW is one of the most promising joining technique which is cost-effective and which has rapid cycle times, in-situ monitoring of weld quality and ability to be automated. Therefore, the theory of USW and process parameters affecting the welding quality are investigated in detailed before the effect of carbon fiber inclusion in polymer system is introduced.

### 2.5.1 Principle of ultrasonic welding

The joining of two parts with USW process is simply provided with applying high frequent mechanical vibrations and static force to outer surface of one of the parts to be welded. The cyclic load from mechanical vibrations causes intermolecular and viscoelastic friction through the thermoplastic material at the welding area. During welding, energy dissipation from the friction is converted to heat which helps to rise the temperature at the joint surface locally. After a short period of time, the temperature is reached at the glass transition for amorphous and semi-crystalline polymers or melting point for crystalline polymers which is sufficient for phase change so that intermolecular diffusion between two parts can take place. After the fusion bonding, the solidification or healing phase is started with a horn (sonotrode) which applies a static pressure to the joint as the cyclic load is not exerted anymore [80].

In order to satisfy the welding process explained above, an electrical signal with a low frequency level is generated from a micro-processor controlled power supply. This low voltage sinusoidal signal is then converted up to 20 or 40 kHz frequency level high voltage signals with the help of piezoelectric ceramic materials covered in the transducer or converter. After then, the ultrasonic vibrations are amplified through the booster which is assembled between transducer and horn. Another duty of booster is to mate the actuation unit comprising converter, booster and horn. The mechanical vibrations are then transferred to the adherends with the part called horn or sonotrode. The design of horn can be changed according to the geometry of welding zone. Furthermore, static force must be applied during welding and solidification phase which is provided with horn. In addition, adherends are should be fixed with clamps and mounted on the custom-made fixture during welding process [81,82]. The schematic illustration of USW components is shown Fig. 2.12 below;

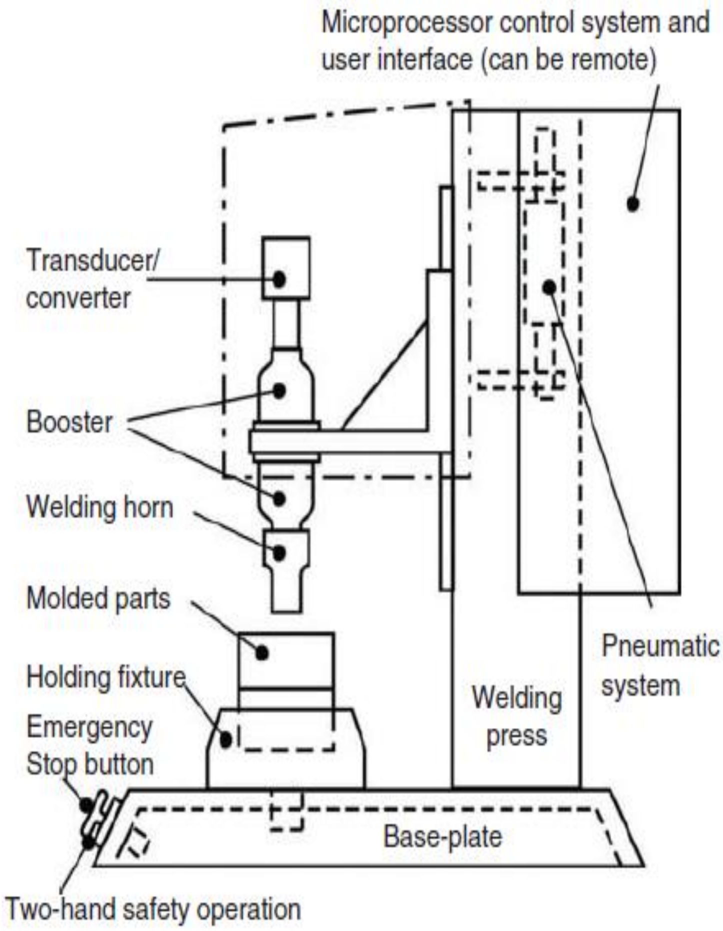


**Figure 2.12** USW process components [81]

## 2.5.2 Joint design and energy directors

The design consideration of joint is important as much as other factors to get reliable, high strength and quality welds. The main factors influencing the joint design are the microstructure of thermoplastic, geometry of part and requirements of application [81]. The most frequent used joint designs including butt joint, lap shear joint and shear joint are demonstrated Fig. 2.13 below;

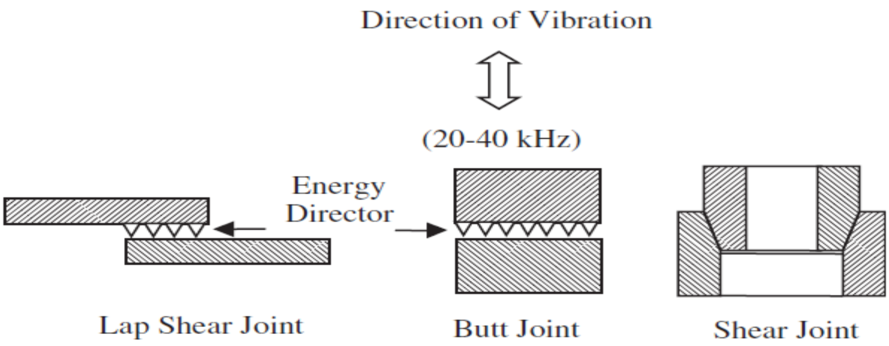


**Figure 2.13** Frequently used joint designs [58]

On the other hand, an energy director (ED) is defined as an extra thermoplastic material placed between two adherends which assists to reduce welding durations and increase efficiency of process as EDs are generally used to localize rapid heating at the joint interface. The aim of using an ED is concentrating the greatest stress at the tip of the ED during welding because this tip has the contact with the surface of the other adherend at the same time. Therefore, polymer starts to melt from the tip of the ED [58,81]. The geometry of the ED can be triangular, rectangular or semi-circular and EDs are pre-molded with the adherend to be joined. However, this analogy is generally used for unreinforced thermoplastic materials [83].

Recently, a new type of ED is introduced and can be used both for SFR-TPC and continuous fiber reinforced thermoplastic composites (CFR-TPC). This flat ED is made of resin layer at which is located between two adherends before welding process. The reason for this requirement is to cut down one manufacturing step of joint and get a stabilized joint strength [84].

In literature, there are several researches available for investigating the effects of geometry and number of ED, traditional ED or flat ED over LSS and other mechanical properties. Villegas et al. [85] studied a research that investigates the effects of geometry, orientation and size of the traditional ED over LSS and welding area with CFR-TPC which is CF/PEI. The main conclusions from the research are that flow of resin is not depended on orientation and dimension of when multiple ED is used, also more than one ED increases overlap welding performance. Besides, LSS is decreased with the resin flash out of overlap area which restricts the number of EDs. Another study from the same author revealed the difference between the traditional triangular EDs and new type of flat EDs. It was found from the power and displacement curves of welding that flat EDs demonstrated similar pattern compared with triangular EDs according to the LSS values and welding process data except for low force and amplitude is necessary [84]. In addition, the influence of ED thickness was investigated by Palardy et al. [83]. The research was again conducted with the material CFR-TPC CF/PEI and it was concluded that thicker EDs performed better performance indicating successful heat generation at the joint interface. Furthermore, the LSS performance of single lap shear joint of CFR-TPC CF/PEEK was investigated with and without flat ED. The main output of this research was that LSS is increased dramatically with the existence of flat ED. It also helped to reduce peak temperature needed for welding [8]. Goto et al. [6] revealed that using flat ED decreases welding energy but increase welding area which enhances LSS and welding quality. Afterall, there is no research found for both investigating the EDs with SFR-TPC in the literature.

### 2.5.3 Ultrasonic welding process parameters

USW has several key process parameters which directly influence the weld strength and quality such as welding duration, welding energy, vertical displacement of sonotrode, amplitude of vibrations, welding pressure or force, solidification time, solidification pressure or force and trigger force [81].

In literature, several studies were performed investigating the effects of these parameters mentioned above both for CFR-TPC and SFR-TPC. Liu et al. [86] used a statistical technique to optimize joint strength of ultrasonically welded glass fiber reinforced nylon 6 composites. Experimental results demonstrated that the amplitude of vibration, solidification time and geometry of ED were found to be the most influential parameters affecting joint strength. The same author performed another research with the same analogy but different matrix. It was revealed from the experiments that the amplitude of vibration, geometry of ED and welding duration were found as the most critical parameters affecting the joint strength of glass fiber reinforced polypropylene [87]. On the other hand, Wang et al. [88] analysed welding characteristics of injection molded SCFR-nylon-6 composite without using ED. Welding energy was established as the most important input value affecting joint quality. However, Villegas [10] reported a different perspective whose aim was to use raw welding process data for optimizing weld strength of CFR-TPC CF/PEI. The maximum joint strength was consistently obtained from monitoring the two welding parameters named dissipated welding power and displacement of sonotrode.

# 3. EXPERIMENTAL METHODS

## *3.1 Specimen Preparation*

ABS polymer (SD-0150W) whose specific gravity is specified as 1040 kg/$m^3$ was supplied from Lotte Advanced Materials, Co with a granular form. On the other hand, chopped strands of short carbon fibers (SCFs) which have a mean diameter of 7µm and filament length of 600µm were provided from ACG Composites, China.

Prior for molding, ABS granules and chopped strands of SCFs were individually placed into an isolated box furnace (Figure 3.1) and kept for drying at least 4h and 80°C [42]. The aim of this process is to eliminate air bubbles and moisture effect on the mechanical properties.

**Figure 3.1** Box furnace

After then, SCFR-ABS composites with variable mixing ratios were prepared according to design of experiment (DOE) conditions explained in the next section. Mixtures were compounded with the help of a melt-mixing screw (Figure 3.2) until reading a constant torque value from the mixer meaning that ABS and SCFs were homogenously mixed.

**Figure 3.2** Melt-mixing screw

Each mixture was transferred into a four-cavity mold rapidly before composite cools down at ambient temperature.  Finally, mixtures containing different SCF fractions were consolidated in hot platen press for 4 min to create dog-bone shaped tensile specimens according to ASTM D638 (Type-IV) [89]. Moreover, unnotched charpy impact test specimens were produced with the same manufacturing conditions but different mold based on ASTM D4812 standard [90]. Finally, molded tensile and impact test specimens are demonstrated in Fig 3.3 below.

**(a)** **(b)**

**Figure 3.3** Molded final specimens of (a) tensile test, (b) impact test

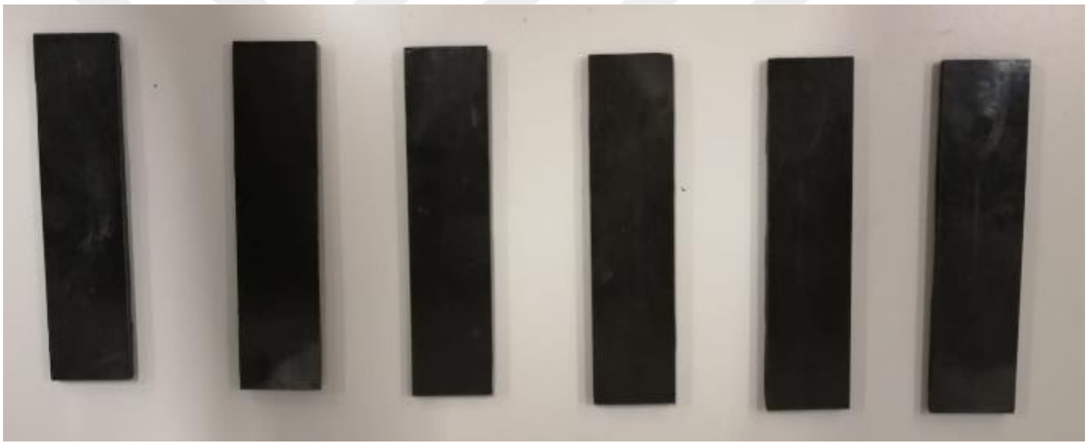

**Figure 3.4** Molded final specimens for ultrasonic welding process

In addition, ultrasonic welded specimens with a specific dimension of 101.6 x 25.4mm were manufactured with the same analogy at the second stage of this study. Molded welding specimens are demonstrated in Fig 3.4.

### *3.2 Design of experiment (DOE) conditions*

At the first stage of this research, molding pressure, molding temperature and carbon fiber content were selected as critical process parameters. In order to save time, cost and effort, Taguchi's $L_9$ ($3^3$) orthogonal array was created for experimental design procedure. Taguchi method is a statistical tool for engineering applications which points out the optimum process parameters of desired output between the pre-defined boundaries. This method basically investigates the quality characteristics of each variable and values them to determine the best process parameters [43,91]. Process parameters and their related levels are indicated in Table 3.1.

**Table 3.1** Control variables and their levels of the first array

| Molding parameter levels | Molding pressure (MPa) | Molding temperature (°C) | Fiber content (%wt.) |
|---|---|---|---|
| 1 | 10 | 200 | 10 |
| 2 | 11 | 220 | 20 |
| 3 | 12 | 240 | 30 |

In the literature, short carbon fibers and ABS polymer were compression molded with a temperature ranging from 200°C and 240°C [1,36]. Therefore, molding temperature levels were assigned according to these studies. Furthermore, fiber loadings starting from 10 percent and having ten percent incremental up to 40 percent were reported at the same study [36]. Similar values were used to compare mechanical response of composites, however 40% fiber loading was omitted due to limitation in the first orthogonal array. Moreover, it was reported that molding pressure was typically varied between 10MPa and 15MPa [92,93]. The fact that the machine has a maximum pressure capacity of 12MPa, the levels were assigned 10, 11 and 12MPa, respectively.

Based on the control parameters for CM of SCFR-ABS composite, $L_9$ ($3^3$) orthogonal array was created and illustrated in Table 3.2. In order to prevent confusion, experiment numbers in the first array (M for compression molding) were named as M1, M2, M3, M4, M5, M6, M7, M8 and M9 respectively.

**Table 3.2** The first Taguchi orthogonal array $L_9$ ($3^3$) for compression molding

| Experiment number | Molding pressure | Molding temperature | Fiber content |
|---|---|---|---|
| M1 | 1 | 1 | 1 |
| M2 | 1 | 2 | 2 |
| M3 | 1 | 3 | 3 |
| M4 | 2 | 1 | 2 |
| M5 | 2 | 2 | 3 |
| M6 | 2 | 3 | 1 |
| M7 | 3 | 1 | 3 |
| M8 | 3 | 2 | 1 |
| M9 | 3 | 3 | 2 |

After all experiments are completed, each value from M1 to M9 was transferred into signal-to-noise (S/N) ratios for analyzing quality characteristics of each process parameter. There are three ways which are smaller is better, nominal the best and larger is better approaches to calculate S/N ratios according to requirement. At this stage of research, mechanical properties of tensile strength, tensile strain at break and absolute impact energy were aimed to investigate. Therefore, larger is better approach was selected and S/N ratio of this approach is expressed in Equation (1);

$$S / N = -10 \log_{10}\left[\frac{1}{n}\sum_{i=1}^{n}\frac{1}{y_i^2}\right] \tag{1}$$

S/N ratios of tensile strength, tensile strain at break and absolute impact energy were calculated and analyzed by Minitab software.

At the second stage of this research, welding performance of SCFR-ABS composite was investigated. Therefore, another orthogonal array of Taguchi $L_9$ ($3^3$) was created. Ultrasonic welding pressure, amplitude of vibrations and welding duration were chosen as crucial control parameters. DOE conditions of ultrasonic welding and their related levels are indicated in Table 3.3. The same analogy was used and experiment numbers in the second array (W for ultrasonic welding) were named W1, W2, W3, W4, W5, W6, W7, W8, and W9 for again preventing conflicts. The second array is demonstrated in Table 3.4.

Lap shear strength (LSS) and welding energy of the ultrasonically welded joints were analyzed. Larger is better approach was chosen for LSS and smaller is better was chosen for welding energy to obtain joints with having higher LSS and consuming minimum energy during welding. Experiment results of LSS and welding energy were transformed to the S/N ratios and analyzed with Minitab software for evaluating the quality performance.

**Table 3.3** Control variables and their levels of the second array

| Molding parameter levels | Welding pressure (MPa) | Amplitude (μm) | Welding duration (sec.) |
|---|---|---|---|
| 1 | 0.20 | 78 | 1 |
| 2 | 0.35 | 87.75 | 1.5 |
| 3 | 0.50 | 97.5 | 2 |

**Table 3.4** The second Taguchi orthogonal array $L_9$ ($3^3$) for ultrasonic welding

| Experiment number | Welding pressure | Amplitude | Welding duration |
|---|---|---|---|
| W1 | 1 | 1 | 1 |
| W2 | 1 | 2 | 2 |
| W3 | 1 | 3 | 3 |
| W4 | 2 | 1 | 2 |
| W5 | 2 | 2 | 3 |
| W6 | 2 | 3 | 1 |
| W7 | 3 | 1 | 3 |
| W8 | 3 | 2 | 1 |
| W9 | 3 | 3 | 2 |

## *3.3 Ultrasonic welding procedure*

At this stage of the study, molded specimens were ultrasonically welded with a 20kHz microprocessor controlled ultrasonic welding machine (Branson 2000iw+) which has a maximum welding power capacity of 2200W and 1:1.5 booster gain ratio. Also, USW was applied to specimens in time-controlled operation mode because welding duration was selected as a variable control factor in the previous section. Moreover, horn with a 50x50mm$^2$ cross-section area and a gain of 1:1.3 was used during welding process.

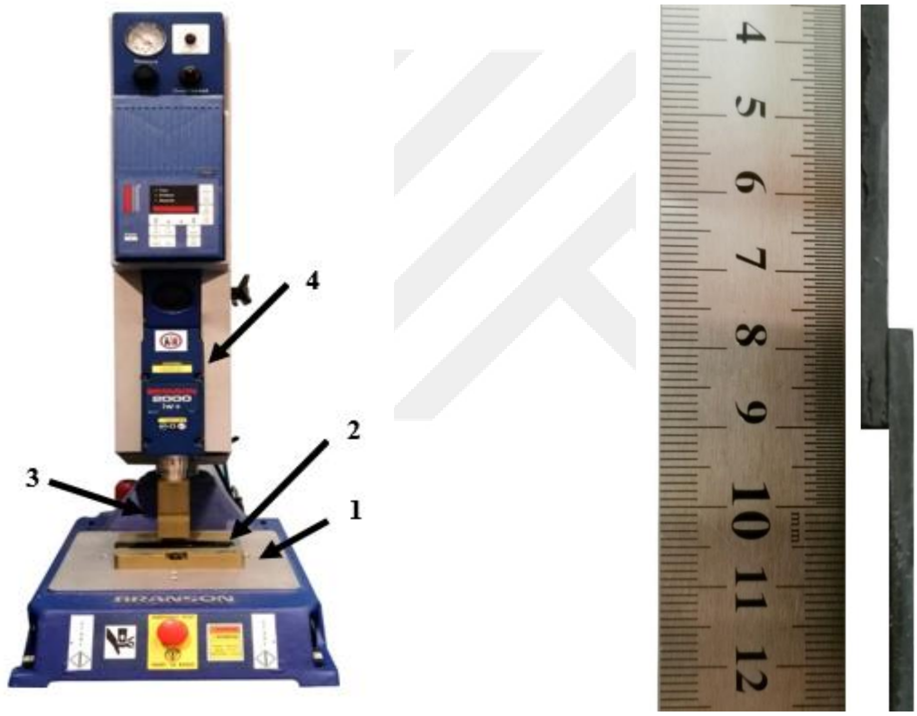


**(a)** **(b)**

**Figure 3.5** (a) USW configuration illustrating the custom-made welding jig (1), the upper and lower adherends (2), sonotrode (horn) (3), the booster section (4), (b) sample joint demonstrating the overlap region

Experiment setup which involves custom-made jig, welding specimens, sonotrode (horn) and booster of welding machine are demonstrated in Fig. 3.5(a). Furthermore, as can be seen from Fig. 3.5(b), specimens were welded under single-lap-shear configuration with a 25.4x12.7mm$^2$ overlap area according to ASTM D3164 [94].

In addition, any type of ED was not used in this stage due to further research considerations. Otherwise, presence of ED would increase the control variables. Trigger force which is expressed as a preload preventing not to slip of adherends before&during welding was kept constant as 200N. Furthermore, solidification time which is the contact period of horn to adherends after welding was selected as 0.2s for each experiment condition. Because the welding machine has a pneumatic system, solidification force which shows the force applied to adherends after welding during solidification time was equal to vibration force. As vibration force (welding pressure times horn cross section) was an indirect variable due to DOE conditions, solidification force changed according to welding pressure.

## *3.4 Mechanical testing and evaluation*

After tensile test specimens were manufactured, samples of each condition based on the first Taguchi array were mechanically tested one by one with INSTRON 8872 according to ASTM D638 test standard to characterize tensile properties of composite. The crosshead speed was chosen as 5mm/min. After that, stress-strain curve of the composite was analyzed by plotting raw data.

For impact properties, 4J of hammer was used for testing unnotched charpy impact test specimens based on ASTM D4812 test standard. After the tests, absolute impact energy of each condition was calculated.

In order to calculate the maximum shear strength which composite withstands with different conditions, the tensile shear tests of welded samples were tested with INSTRON 8872 according to ASTM D3164 test standard. The crosshead speed was 1.3mm/min and the test setup is demonstrated in Fig. 3.6. Furthermore, in order to reduce effect of bending during testing, centerline misalignment of tensile load path which is a result of single-lap configuration [95] was adjusted with two identical additional plastic parts in both grips and single lap shear configuration is shown in Fig. 3.7. In addition, LSS of each condition from the second array was calculated as dividing the maximum shear load over 322.58 $mm^2$ constantly [10].

At least three samples were prepared and performed for tensile, impact and welding tests covering all conditions stated in both experimental design arrays.

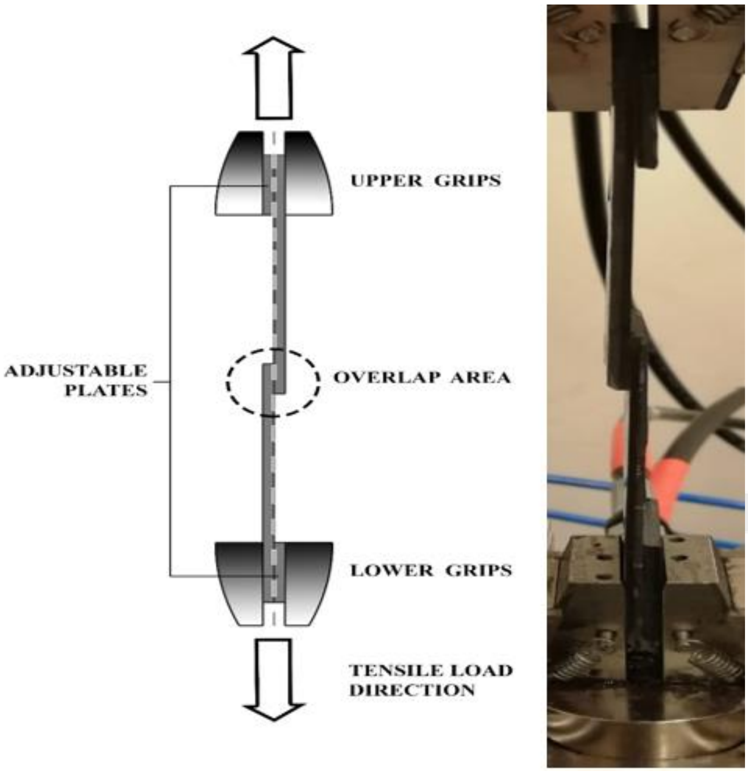


**Figure 3.6** Tensile shear test of welded specimens

## *3.5 Analysis of fracture surfaces*

In order to characterize microstructure of fractured surfaces from tensile, impact and welded specimens, a small piece of sample from fractured surface was examined in scanning electron microscopy (SEM) with an accelerating voltage of 15kV. The microstructure of composite was analyzed on focusing on the maximum and minimum value of each mechanical property for better characterization.

# 4. MECHANICAL RESPONSE OF COMPRESSION MOLDED SCFR-ABS COMPOSITE

## *4.1 Effect of molding parameters on the mechanical properties*

As it was referred earlier, the first stage of this research illustrates the mechanical response of compression molded SCFR-ABS composite under several control parameters with different levels. After mechanical tests, the stress-strain curve of the samples with the best result of each condition according to Table 3.2 was generated and demonstrated in Fig. 4.1. Moreover, average results of tensile and impact test properties are tabulated in Table 4.1.

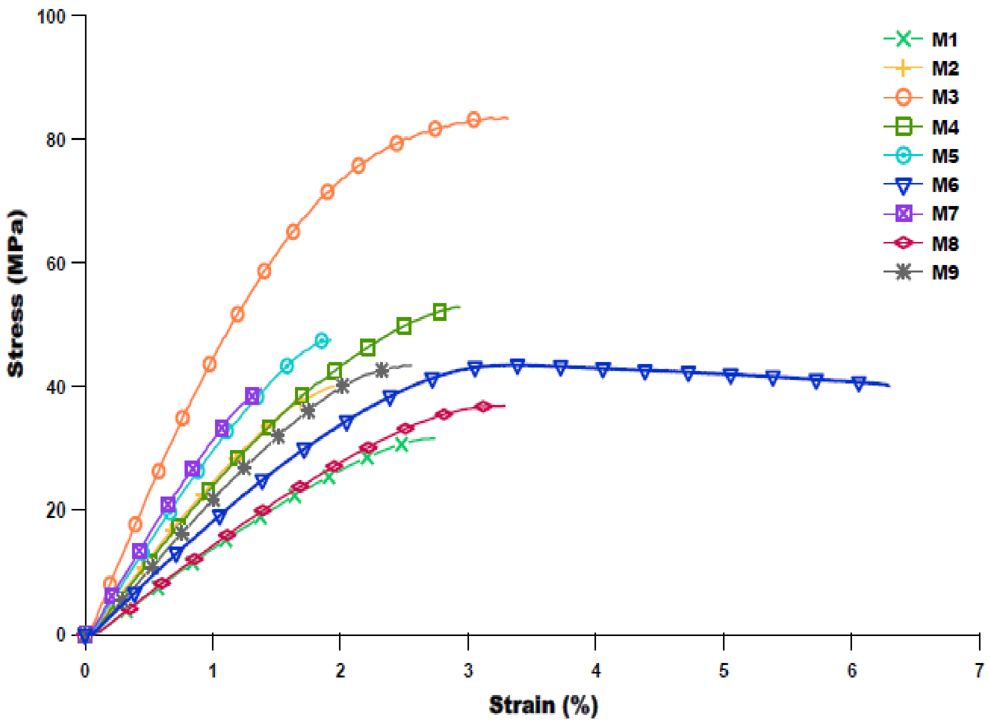


**Figure 4.1** Tensile stress-strain curve for the compression molded SCFR-ABS

**Table 4.1** Mechanical properties of the compression molded samples

| Experiment Number | Tensile strength (MPa) | Tensile strain (%) | Impact energy (J) |
|---|---|---|---|
| **M1** | 30.93 | 2.64 | 0.66 |
| **M2** | 40.62 | 2.04 | 0.59 |
| **M3** | 74.98 | 2.95 | 0.69 |
| **M4** | 46.56 | 2.90 | 0.70 |
| **M5** | 47.35 | 2.29 | 0.50 |
| **M6** | 42.00 | 5.54 | 0.72 |
| **M7** | 38.21 | 1.43 | 0.38 |
| **M8** | 37.88 | 4.35 | 0.45 |
| **M9** | 42.97 | 2.52 | 0.58 |

According to the Fig. 4.1, the maximum tensile strength was achieved from the M3 samples. The M3 condition distinguished from others reaching around 85MPa tensile strength with 3.5% tensile strain. On the contrary, the highest ductility of about 6.5% was observed from the M6 samples. Despite M3 and M6 share the same molding temperature and have a small difference in molding pressure, the striking difference is that M3 has higher carbon fiber content than the M6 samples. As expected, tensile strength of composite was mostly influenced by reinforcement content in matrix. In literature, similar results were also reported on the effect of fiber content for strength enhancement in thermoplastic composites [3,36,41,42]. Furthermore, brittle behavior due to the higher fiber stiffness was observed for reinforced composites although tensile strength improvement was succeeded with increasing carbon fiber content [3,42]. The main effects plot of S/N ratios for tensile strength demonstrates this difference in detailed (Fig. 4.2).

Fig. 4.2 also provides the details of the effect of compression molding temperature and pressure on the strength of SCFR-ABS composite as there is a deficiency about this parameters in literature. With respect to Fig. 4.2, tensile strength of composite is positively affected by increasing carbon fiber content and molding temperature. Furthermore, the importance of molding pressure on the tensile strength is less compared with other control parameters. The influences of control parameters can also be deduced from comparing the gradients of the main effects plot for tensile strength (Fig. 4.2). The significance of carbon fiber content and molding temperature is proved from the plots that higher slopes increase the importance on tensile strength.

Although M3, M5 and M7 conditions share the same carbon fiber content, it was observed that tensile strength was dramatically improved when molding temperature is shifted from level 1 to 3. However, increasing molding pressure demonstrated a negative effect. Moreover, M1 samples having the lowest molding temperature and carbon fiber content indicated the minimum average tensile strength value of 30.93MPa. Furthermore, the strength ratio of M3 to M1 samples was found to be more than 2.5 times demonstrating the significance of process parameters once more. It was concluded that the highest tensile strength was determined from the parameters of molding pressure of 11MPa, molding temperature of 240°C and fiber content of 30% (highlighted with a circle in Fig. 4.2). The only difference between processing parameters of M3 and best condition was shifting pressure level from 10MPa to 11MPa. Although it was expected to get higher tensile performance after analysis, 77.1MPa tensile strength was observed. In fact, this unexpected result was observed due to increased non-linear deformation ability of matrix and excessive interaction between fibers causing interfacial microfailure around fibers [96].

The maximum strain at fracture was observed from the M6 sample whose processing parameters were molding pressure of 11MPa, molding temperature of 240°C and fiber content of 10% (Table 4.1). Furthermore, approximately 50% drop in ductility concluded from shifting the carbon fiber content from level 1 (10%) to level 3 (30%) as expected. The ductile to brittle transition in reinforced composites is attributed to the higher fiber stiffness as compared to that of the matrix [3,41,42,96]. According to this finding, ductility improvement was provided with decreasing fiber content. Moreover, the effect of molding temperature on tensile strain was found as crucial compared with molding pressure. It can also observed from the S/N ratio plots that gradient of molding temperature is higher than molding pressure (Fig. 4.3). It was concluded that M6 had the best conditions according to the experimental design analysis and there was no need to conduct any confirmation experiment.

For the impact properties, the optimum impact energy can be attained by a molding pressure of 10MPa, molding temperature of 240°C and carbon fiber content of 20%. However, this parameter set was not included in the first Taguchi orthogonal array. Therefore, a confirmation experiment satisfying this condition was done yielding an impact energy of 0.74J. The impact energy of verification sample confirmed a slight increase than the highest value reported for the M6 sample (Table 4.1), displaying the effectiveness of the experimental design methodology. Furthermore, despite M3 and M6 sharing the same level of molding temperature, only 5% drop in impact energy was observed. This can be expressed by although M3 has decreased tensile strain value, its high strength tolerates for a decent impact energy. Moreover, the most influential parameter was found as molding pressure demonstrated by the main effects plot (Fig. 4.4).

Crack growth of fiber-reinforced thermoplastics under impact loadings is much faster than virgin polymers due to accelerated crack propagation stemming from stress concentration at fiber tips [97]. Therefore, samples with lower fiber content are typically expected to display higher impact energy. This holds true for M6 samples with the lowest fiber content. Relatively high energy of M3 samples with high fiber content presents an exception indicating the influence of other processing parameters governing the impact response.

ANOVA is a widely used statistical method to determine impacts of each control factor with their contribution upon the outcome of an experiment. The significance of the process parameters were investigated with a 95% confidence level. For tensile strength, fiber content, molding temperature and molding pressure contributed 31.55%, 25.99% and 11.71%, respectively (Table 4.2). For tensile strain at break, fiber content, molding temperature and molding pressure contributed 38.68%, 34.93% and 18.55%, respectively (Table 4.3). For impact energy, fiber content, molding temperature and molding pressure contributed 16.35%, 30.01% and 50.39%, respectively (Table 4.4). These results are in line with the trends exhibited in the mean effects plots (Fig. 4.2, Fig. 4.3, Fig. 4.4).

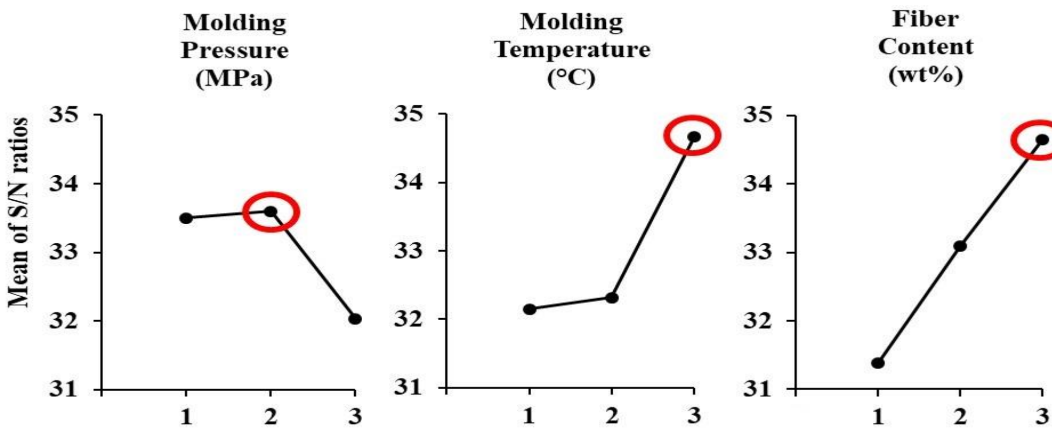


**Figure 4.2** Main effects plot of S/N ratios for tensile strength (Larger is better)

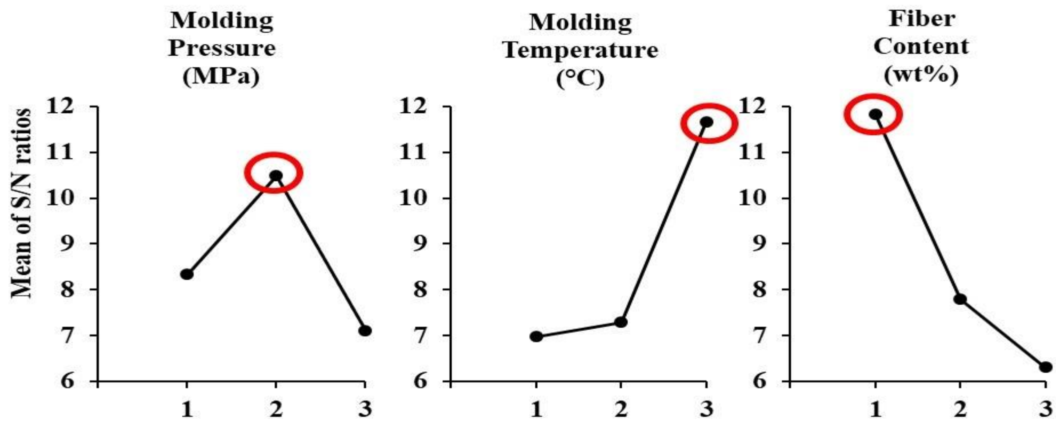


**Figure 4.3** Main effects plot of S/N ratios for tensile strain at break (Larger is better)

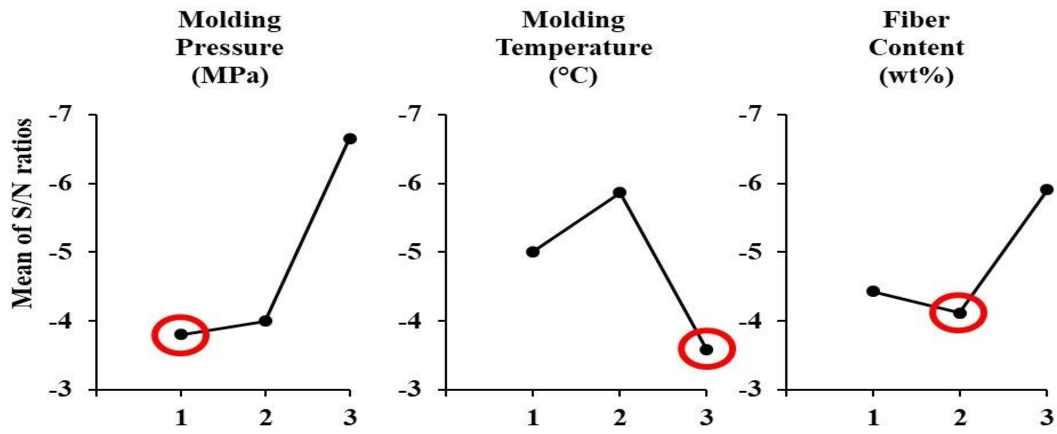


**Figure 4.4** Main effects plot of S/N ratios for impact energy (Larger is better)

**Table 4.2** ANOVA table for tensile strength

| Factors | Degree of freedom (DF) | P-value | Significance % |
|---|---|---|---|
| Molding pressure | 2 | 0.724 | 11.71 |
| Molding temperature | 2 | 0.542 | 25.99 |
| Fiber content | 2 | 0.494 | 31.55 |
| Error | 2 | | 30.75 |
| Total | 8 | | 100 |

**Table 4.3** ANOVA table for tensile strain at break

| Factors | Degree of freedom (DF) | P-value | Significance % |
|---|---|---|---|
| Molding pressure | 2 | 0.297 | 18.55 |
| Molding temperature | 2 | 0.183 | 34.93 |
| Fiber content | 2 | 0.169 | 38.68 |
| Error | 2 | | 7.84 |
| Total | 8 | | 100 |

**Table 4.4** ANOVA table for absolute impact energy

| Factors | Degree of freedom (DF) | P-value | Significance % |
|---|---|---|---|
| Molding pressure | 2 | 0.060 | 50.39 |
| Molding temperature | 2 | 0.097 | 30.01 |
| Fiber content | 2 | 0.165 | 16.35 |
| Error | 2 | | 3.25 |
| Total | 8 | | 100 |

## *4.2 Fracture morphology analysis of compression molded samples*

Microstructural studies focused on characterizing the striking properties on the fracture surfaces of samples exposed to tensile and impact loadings. For the clearance of comparison, samples having the highest and the lowest tensile strength (Fig. 4.5, Fig. 4.6, Fig. 4.7) and impact energy (Fig. 4.8, 4.9) in Table 4.1 were examined. First of all, it is clear that for all samples, discontinuous fibers were mixed homogenously and randomly oriented within the polymer matrix. It can be clearly understood from Fig. 4.5a that the general trend of fibers in M1 sample were pull-out from the matrix indicating weak interfacial adhesion. Fiber pull-out is a clear sign of micro failure in short fiber reinforced composites due to plastic deformation of the matrix under tensile straining [47,96]. For that matter, adhesion enhancement beween the fiber and matrix has been studied for improving the tensile performance [42,96]. Another reason is that carbon fibers are less likely to interact with the majority of polymers due to having non-polar surfaces which results a weak interfacial bonding strength between the fiber and matrix [98].

Fiber pull-out from the matrix was also observed with a decreased level in the M3 sample which has the highest tensile strength compared with the M1 samples. Moreover, Fig. 4.6b clearly revealed that increasing the level of molding temperature from level 1 to level 3 develops an improvement in polymer-fiber bonding. In fact, wettability of fiber by ABS matrix depends on the surface free energy of fiber and matrix. The surface energy of fiber should be higher than the matrix in order to obtain better wetting of fiber by matrix. [99]. According to the SEM images, increasing molding temperature improved the wetting of fiber by matrix as the fibers were surrounded with matrix after failure. This means that the difference of surface energies between fiber and the matrix molded at 240°C shall be greater than the difference of surface energies between fiber and the matrix molded at 200°C. Furthermore, pull-out of carbon fibers from the matrix created dark rings at the interface in all samples revealed in the magnified images (Fig. 4.5, Fig. 4.6, Fig. 4.7) [42,44].

M1 samples exhibited a higher number of pores than that of M3 samples due to insufficient interfacial adhesion as illustrated in Fig. 4.6b. It is previosly mentioned that the number and morphology of pores due to debonding directly affects the tensile properties of thermoplastic composites [36]. Increasing molding temperature from 200°C to 240°C positively affects the tensile strength with apparent indication of better interfacial bonding on the fiber surface as shown in Fig. 4.6b. Fig. 4.7b also hints at a higher deformation level in the matrix and thus can be related with the improved ductility of this sample.

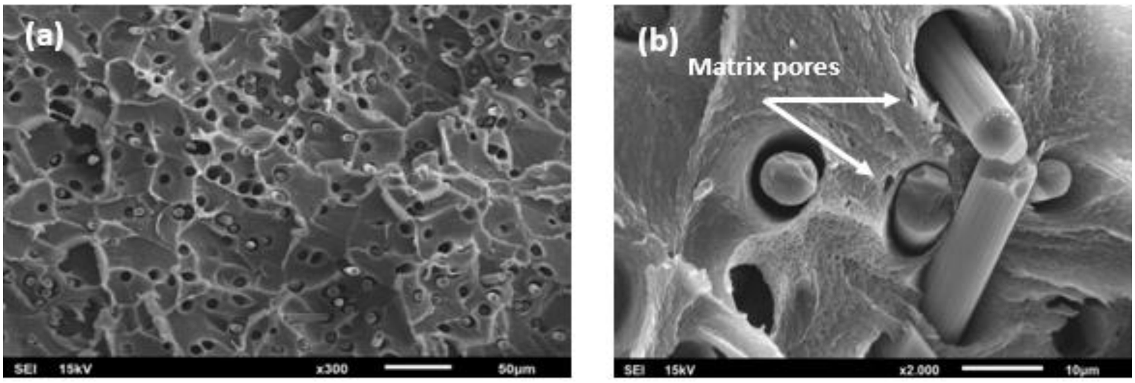


**Figure 4.5** Fracture surface images from (a) M1 with x300 magnification, (b) M1 with x2000 magnification

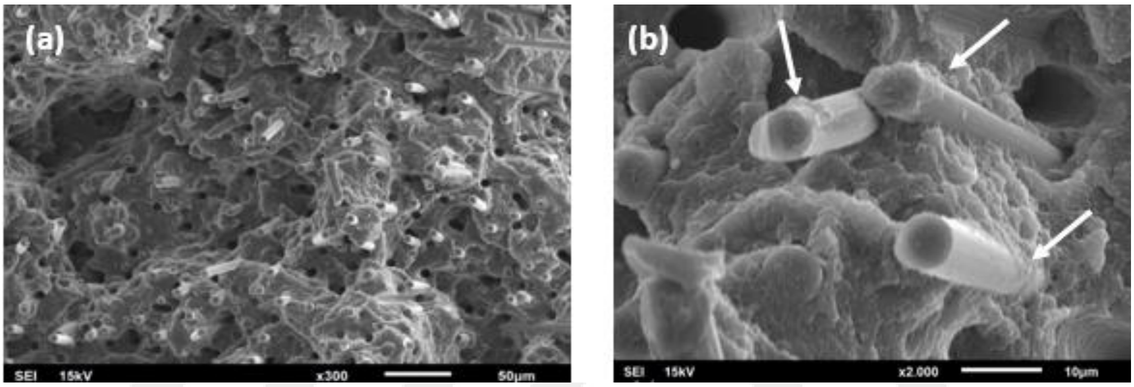


**Figure 4.6** Fracture surface images from (a) M3 with x300 magnification, (b) M3 with x2000 magnification

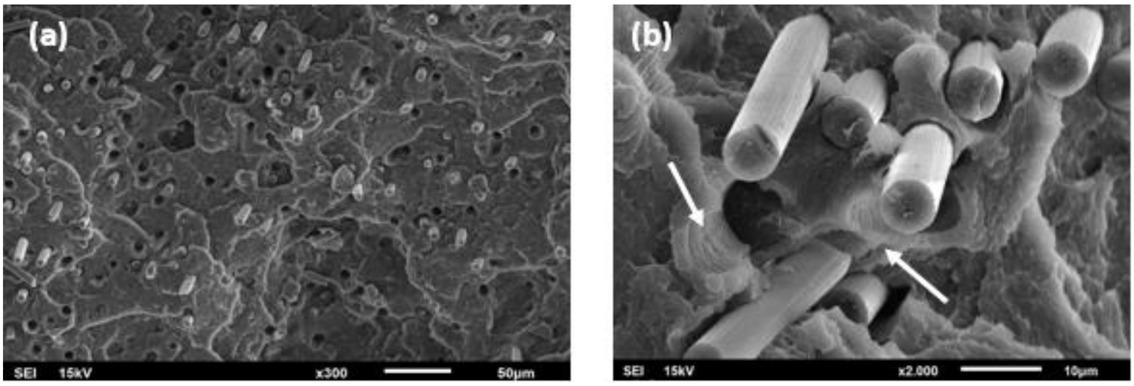


**Figure 4.7** Fracture surface images from (a) M6 with x300 magnification, (b) M6 with x2000 magnification

Unnotched charpy impact energy is the total energy absorption of a material during fracture initiation and crack propagation [100]. In contrast to tensile loading, matrix indicates a shear type failure associated with the Charpy configuration. Therefore, the main mechanism of fracture during impact is expressed as debonding and pull-out of fibers (Fig. 4.8, Fig. 4.9). Fiber to fiber interaction was observed severely in M7 due to its higher fiber content as compared with that of M6, increasing stress concentration zones throughout the matrix leading to easier initiation of fracture.

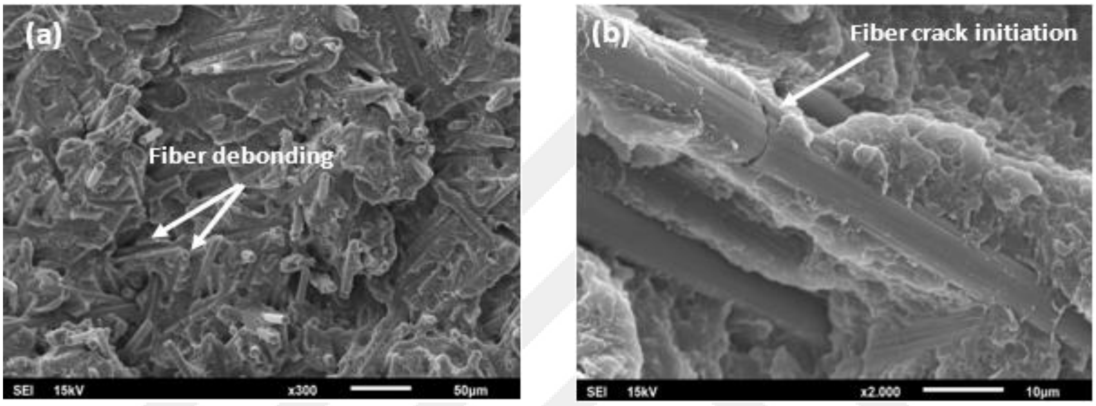


**Figure 4.8** Fracture surface images of impact test samples from (a) M7 with x300 magnification, (b) M7 with x2000 magnification

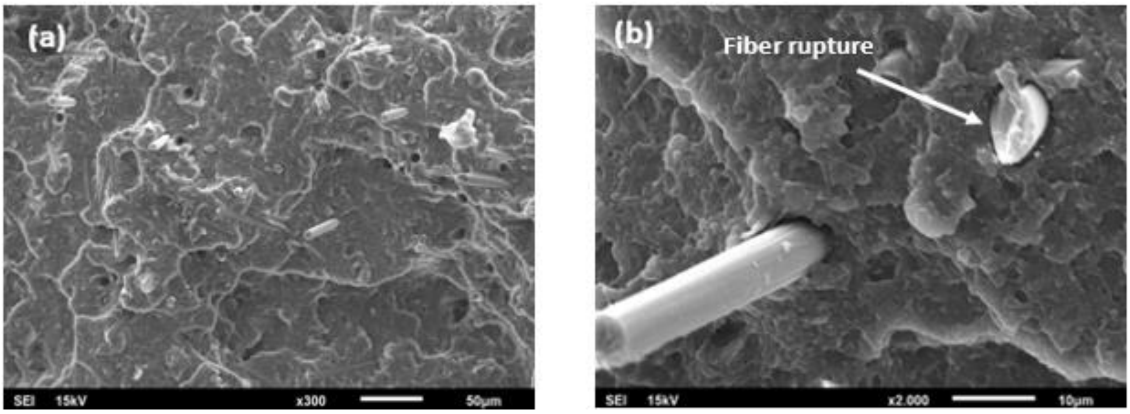


**Figure 4.9** Fracture surface images of impact test samples from (a) M6 with x300 magnification, (b) M6 with x2000 magnification

Moreover, fibers are debonded or pulled-out due to poor interfacial strength between fibers and matrix as observed in Figs. 4.8a, 4.9a. On the other hand, fiber rupture occurs when fiber-matrix interfacial strength between fiber and matrix is greater than the strength of fiber itself (Fig. 4.9b) [96].

On the other hand, the impact energy of composite also depends on fiber length. Longer fibers absorb more energy than shorter fibers as the number of fiber ends decreases which cause stress concentration zones resulting in defects [101]. Therefore, as molding pressure increases, it is more likely to happen that fiber lengths are reduced decreasing the impact absorption capacity. Furthermore, the stress generated at fiber tips decreased with low-pressure level influencing the impact energy positively.

## *4.3 Summary on the mechanical response of compression molded SCFR-ABS composite*

In this chapter, effects of processing parameters on the mechanical response of SCFR-ABS composite with an experimental design approach were investigated. In addition, fracture morphology analysis of tensile and impact samples was carried out with the following conclusions.

1. Increasing carbon fiber content and molding temperature of composite resulted in an enhancement of tensile strength. It can be referred from the main effects plot that the highest levels of these control parameters demonstrated the highest strength. Therefore, carbon fiber content and molding temperature were determined as the most significant control parameters influencing tensile properties.
2. Impact energy of composite depended mostly on molding pressure whose contribution was found as 50.39%. It was also pointed out that the decreasing pressure levels improved the impact properties. Furthermore, carbon fiber content was found to have the limited effect of 16.35% over impact energy.

3. According to observations from fracture surface analysis, fibers pull-out from the matrix was considered as the main fracture mechanism of compression molded samples indicating poor interfacial adhesion between fibers and matrix.

# 5. MECHANICAL RESPONSE OF ULTRASONIC WELDED SCFR-ABS COMPOSITE

## 5.1 Effect of welding parameters on the joint strength

The second part of this research focused on investigating the influences of USW parameters on the LSS of SCFR-ABS composite joints while optimizing the energy dissipation during welding. For this reason, the second Taguchi orthogonal array was created as listed previously in Tables 3.3, 3.4. According to the results from Chapter 4, tensile strength was affected by molding pressure less severe who had a contribution of around 11%. However, the influence of molding pressure on the impact energy was more dominant who had a contribution of over 50%. In order to satisfy concomitant strength and impact energy superiority, the first level condition (10MPa) of molding pressure, optimum carbon fiber content and molding temperature were selected although 11MPa of molding pressure was the optimum value. Accordingly, all the samples to be welded were prepared with the compression molding conditions of 10MPa pressure, 240°C temperature and 30% carbon fiber content.

After mechanical tests, average results of LSS, welding energy and their corresponding ratios for each condition are tabulated in Table 5.1.

**Table 5.1** Mechanical response of welded specimens

| Experiment Number | LSS (MPa) | Welding energy (J) | LSS/Welding energy (LSS/kJ) |
|---|---|---|---|
| **W1** | 6.64 | 825 | 8.04 |
| **W2** | 7.67 | 1897.5 | 4.04 |
| **W3** | 5.92 | 2640 | 2.24 |
| **W4** | 5.12 | 1237.5 | 4.13 |
| **W5** | 2.78 | 2860 | 0.97 |
| **W6** | 6.42 | 1925 | 3.34 |
| **W7** | 2.86 | 2200 | 1.30 |
| **W8** | 2.37 | 1595 | 1.48 |
| **W9** | 3.82 | 2640 | 1.45 |

A typical load-displacement curve which demonstrates the mechanical response of lap joints under shear loading is demonstrated in Fig. 5.1. This curve was generated from the best results of each condition. Joint stiffness and ultimate strength are probed as they represent the critical features for load-bearing components [102]. It can be asserted that all the samples exhibit a linear response followed by fracture at the ultimate strength level. This type of response is typical in previos studies [6,102,103]. However to our best knowledge, this is the first work where such mechanical behavior is shown for randomly oriented discontinuous fiber reinforced thermoplastic composites welded with ultrasound.

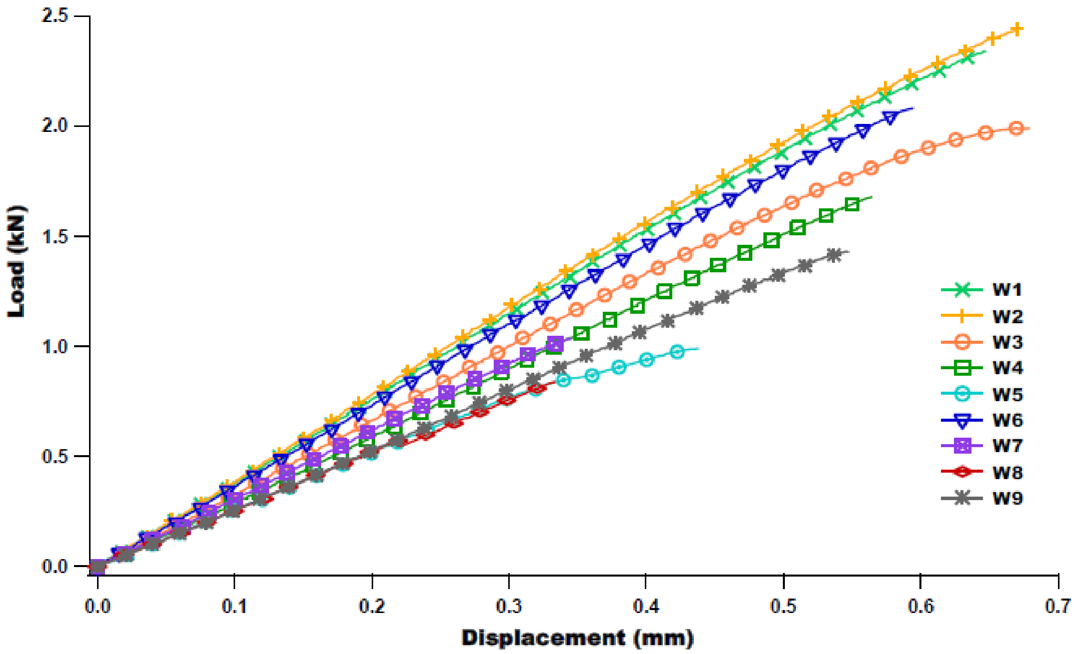


**Figure 5.1** Load versus displacement curves for single lap shear configuration tests

According to the control parameters for welding, the mechanical response character does not vary significantly which also can be deduced from Fig. 5.1. Although this disadvantage, the significance of each control parameter was given effort to be defined by a similar statistical approach as followed in Chapter 4 for optimizing the LSS. As outlined in Fig. 5.2, the highest LSS of 7.67MPa was obtained from sample W2 welded at 0.20MPa pressure and 87.75µm amplitude for a duration of 1.5s. However, the minimum LSS value of 2.3MPa was observed in sample W7 with a welding condition of 0.5MPa pressure, 78µm amplitude and 2s welding duration. The large difference between the maximum and minimum values proves the importance of process parameters for manufacturing enhanced joints.

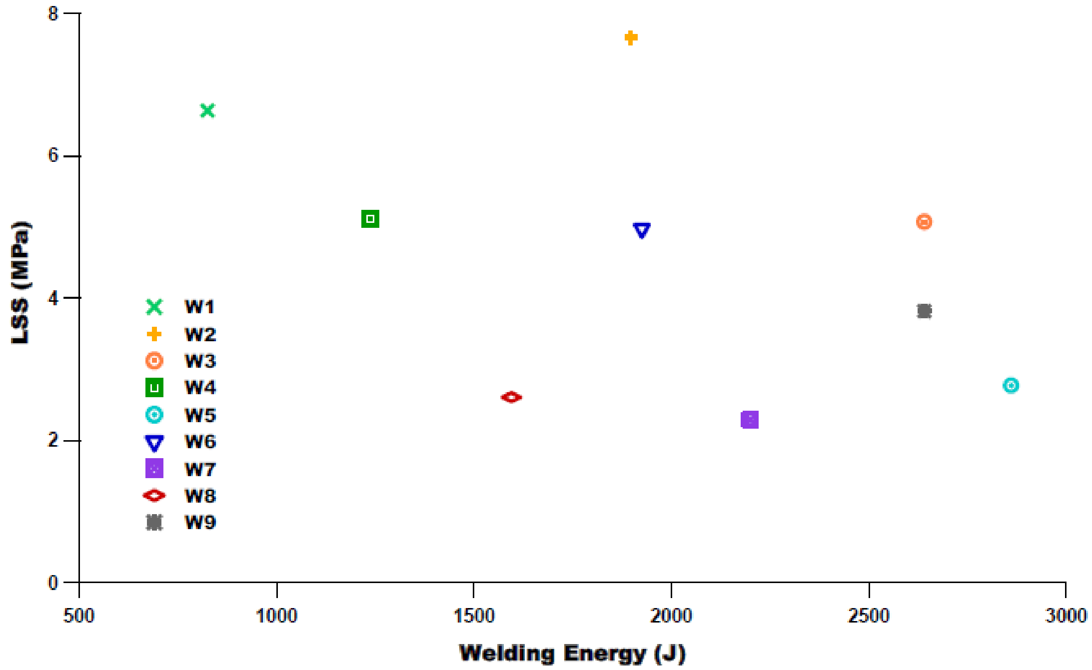


**Figure 5.2** LSS versus welding energy optimization plot

For estimating the influence of welding pressure, amplitude and welding duration on LSS, ANOVA with a 95% confidence level was carried out to determine the percentage contributions. As such, welding pressure had the highest significance with 70.23% followed by welding duration with 25.97%. Although the maximum LSS was achieved for sample W2, the main effects plots in Fig. 5.3 indicate that the optimum parameters are 0.2MPa welding pressure, 97.5µm amplitude and 1.5s welding duration. This set of parameters is indeed very similar to that used for fabricating the W2 sample with the exception of a slight difference in peak-to-peak amplitude, which is shown to have minor significance (less than 5%). On the other hand, W9 sample also shares the same amplitude and welding duration with the optimum parameter set. Nevertheless, variation in the welding pressure led to a dramatic decrease in the LSS of this sample pointing to its strong influence on the process outcome. This can also be delineated by the gradients of the main effects plot for lap shear strength (Fig. 5.3).

Energy dissipation is another key factor in the ultrasonic welding process and energy minimization must be tracked while improving the joint strength. A study about welding properties of SCFR-nylon 6 composite exhibited that if welding energy exceeds a certain threshold value, the lap area is over-welded. This also leads to polymer degradation and bonding efficiency decreases [88]. Thus, the purpose herein is the minimization of energy dissipation while maintaining high LSS. Accordingly, the minimum energy dissipation of 825J was recorded during the fabrication of sample W1, which has a parameter set of 0.2MPa welding pressure, 78µm amplitude and 1s welding duration. In contrast, 2860J as the maximum energy was obtained in sample W5, with a parameter set of 0.35MPa welding pressure, 87.75µm amplitude and 2s welding duration. Furthermore, although W1 did not possess the highest LSS value, the most effective LSS over welding energy ratio was obtained from this sample. In fact, W1 dissipated 825J energy during welding demonstrating its energy-saving characteristic. Therefore, this condition may be preferred depending on operational requirements.

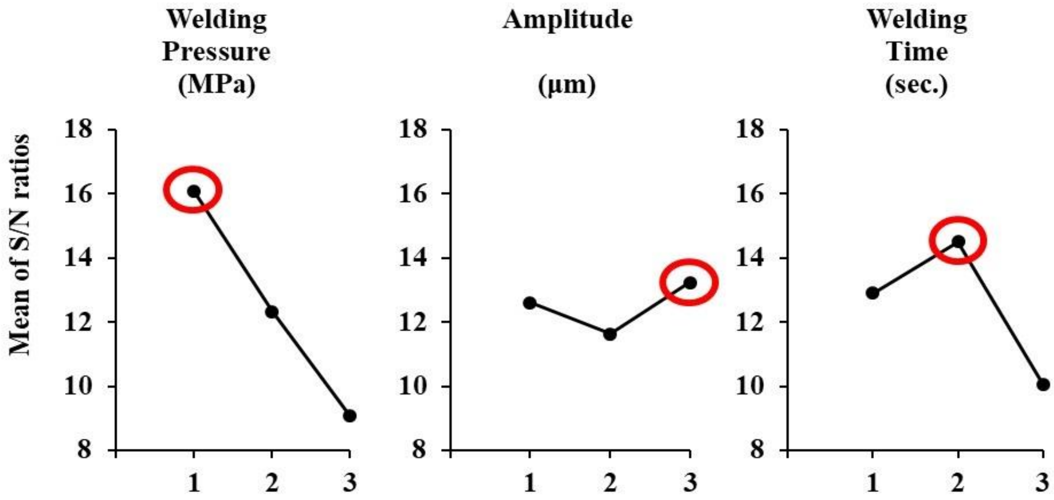


**Figure 5.3** Main effects plot of S/N ratios for LSS (Larger is better)

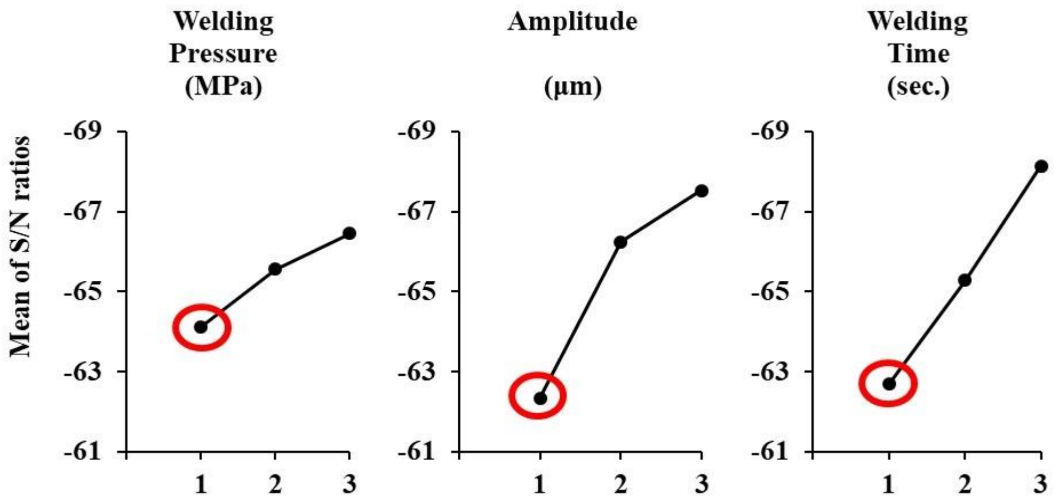


**Figure 5.4** Main effects plot of S/N ratios for welding energy (Smaller is better)

It is obvious from the main effects plot (Fig. 5.4) that increased levels of all control factors lead to high energy consumption. In addition, since welding duration is linearly proportional to welding energy, a similar change is expected in dissipated energy with increased duration. In practice, a two-fold increase in welding duration (W1 versus W5) led to about 2.5 times more dissipated energy, indicating the effect of other factors, notably amplitude. In fact, ANOVA study demonstrates that the two most significant parameters for welding energy were welding duration with 50.56% and amplitude with 40.89%.

**Table 5.2** ANOVA table for LSS

| Factors | Degree of freedom (DF) | P-value | Significance % |
|---|---|---|---|
| Welding pressure | 2 | 0.042 | 70.23 |
| Amplitude | 2 | 0.819 | 0.69 |
| Welding duration | 2 | 0.107 | 25.97 |
| Error | 2 | | 3.11 |
| Total | 8 | | 100 |

**Table 5.3** ANOVA table for welding energy

| Factors | Degree of freedom (DF) | P-value | Significance % |
|---|---|---|---|
| Welding pressure | 2 | 0.390 | 5.22 |
| Amplitude | 2 | 0.075 | 40.89 |
| Welding duration | 2 | 0.062 | 50.56 |
| Error | 2 | | 3.33 |
| Total | 8 | | 100 |

It can also be recognized that LSS and energy dissipated are not positively correlated. It is possible to identify the welding parameters leading to high LSS with low energy dissipation as a crucial outcome of this work. For instance, sample W2 with the highest LSS has a welding energy level lower than the majority. It is also important to mention that LSS decreased dramatically above a threshold energy level, causing thermally induced structural degradation of the composite. It is envisaged that utilization of energy directors may help accumulate heat on the overlap area providing controlled welding and improved LSS.

## *5.2 Fracture morphology analysis of welded samples*

The fracture surfaces of samples bearing highest (W7) and lowest (W2) LSS levels are represented herein. The failure mode of a polymer is closely related with the type of loading, loading rate and temperature [104]. In addition, process induced thermal effects may also be influential due to polymer degradation and related microstructural variations. In the specific case of ABS, degradation process occurs when the polymer is exposed to excessive heat and oxygen resulting oxidation which leads to premature failure [105]. On the other hand, by the nature of USW, local temperature in the bonding layer of the joint over-lap regions may rise high enough to overheat the polymer chain causing undesirable outgassing. Therefore, pores are generated at the heat affected zone (HAZ) for sufficiently high welding energy levels [88]. Increasing welding pressure and welding energy up to a critical value improves interfacial bonding efficiency of joints [88]. However, once temperature of HAZ exceeds its critical value, polymer chains are chemically unbonded, pores are generated decreasing bonding efficiency resulting LSS. Fig. 5.5 clearly displays the post-welding generated pores negatively affecting the joint lap shear reponse. In contrast, the pre-welding zone is noticeably pore free.

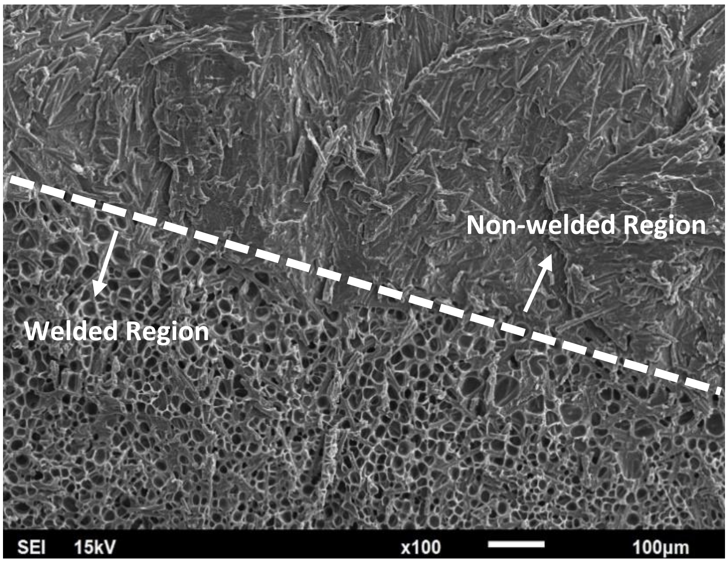


**Figure 5.5** Fracture surface images of welded vs. non-welded region from W2

Moreover, detailed fractured surfaces are expressed in Figs. 5.6, 5.7 revealing different failure modes for joints W2 and W7 in a comparative manner. Fracture behavior of joints can be categorized into three, namely interfacial separation, nugget shear fracture and nugget pull-out modes which can also be correlated with welding energy [106]. A typical nugget shear fracture mode was observed in W2 joint demonstrating the highest LSS while dissipating close to 1900J during welding as shown in Fig. 5.7b. However, overheating due to increased welding duration and especially welding pressure led to structural degradation of the composite along with a low LSS and welding energy of 2200J (Fig. 5.6b). Thus, nugget pull-out fracture mode was observed in W7 joint.

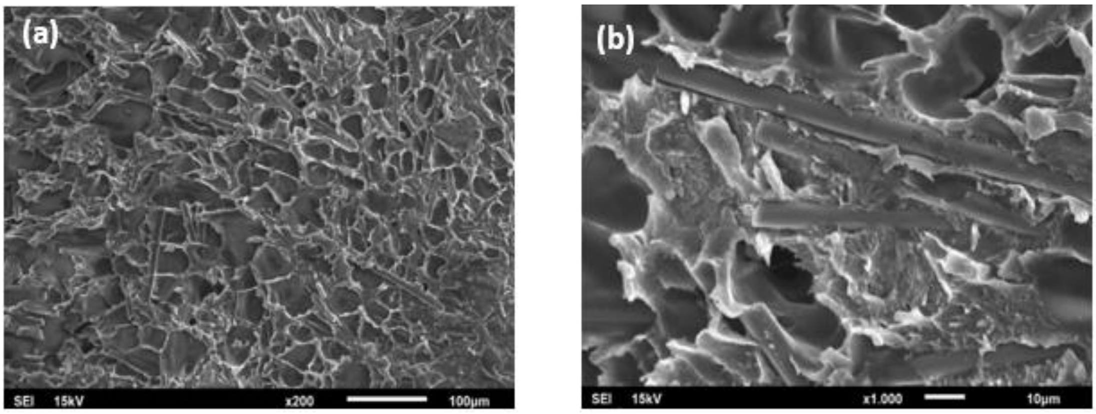


**Figure 5.6** Fracture surface images from (a) W7 with x200 magnification, (b) W7 with x1000 magnification

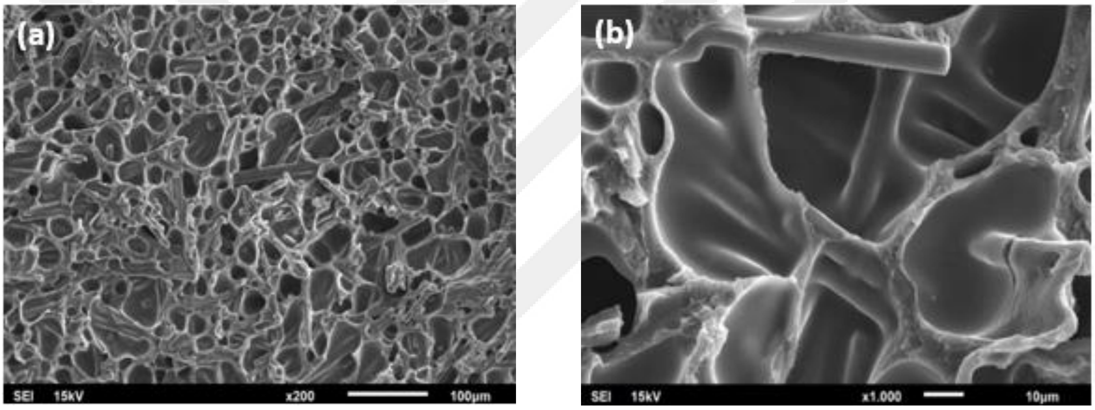


**Figure 5.7** Fracture surface images from (a) W2 with x200 magnification, (b) W2 with x1000 magnification

On the other hand, variation in fracture surface morphology with respect to energy dissipation is demonstrated in Figs. 5.8, 5.9. For the lowest welding energy level of 825J, interfacial seperation failure mode was observed. Increased time and pressure in joint W5 resulted in a natural outcome of higher energy dissipation, promoting the appearance of relatively longer fibers on the fracture surface (Fig. 5.9b). As seen in Fig. 5.9b, these fibers were seen to indicate a lack of interfacial adhesion due to the difference in the melting temperature of ABS and carbon fiber.

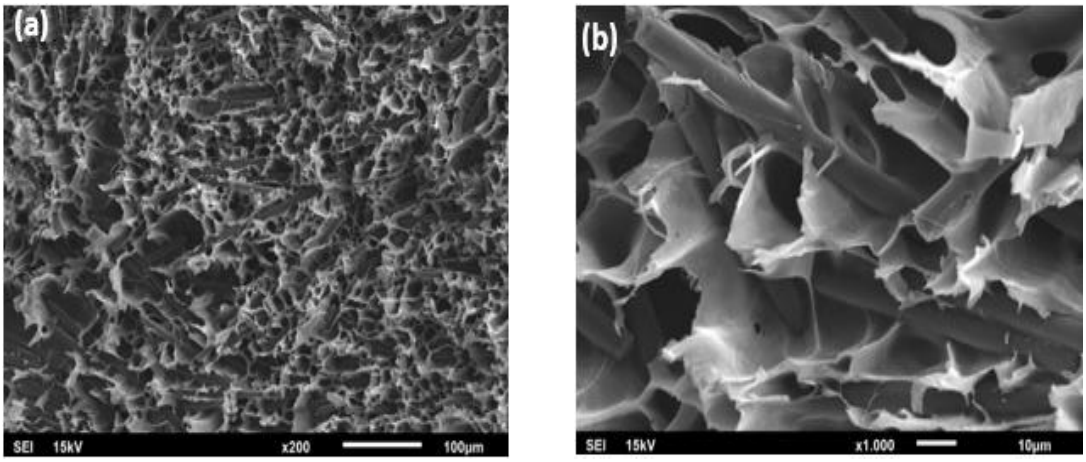


**Figure 5.8** Fracture surface images from (a) W1 with x200 magnification, (b) W1 with x1000 magnification

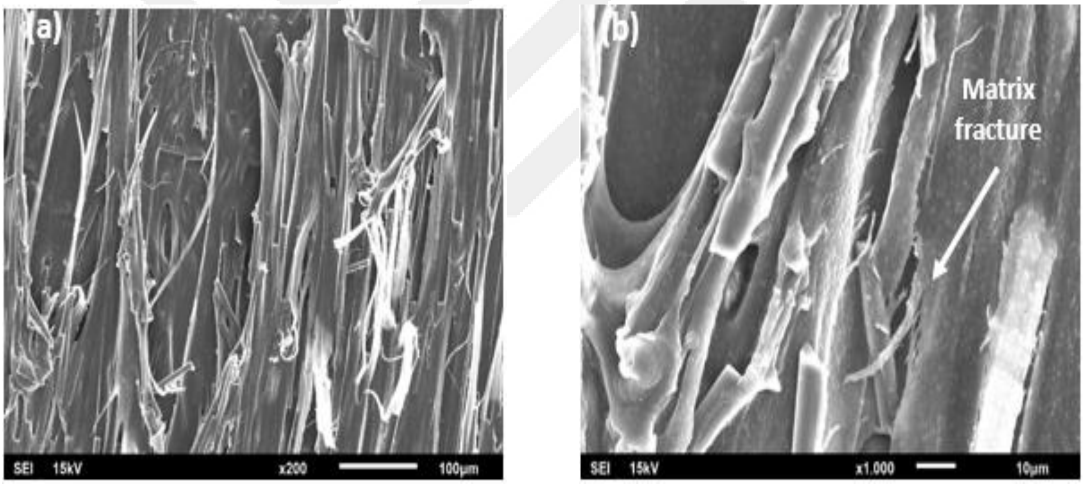


**Figure 5.9** Fracture surface images from (a) W5 with x200 magnification, (b) W5 with x1000 magnification

## *5.3 Summary on the mechanical response of ultrasonic welded SCFR-ABS composite*

In this chapter, the influences of USW processing parameters namely welding pressure, amplitude and welding duration on the mechanical performance and welding energy of SCFR-ABS composite with another experimental design approach were investigated. Moreover, fractured surface analysis of welded samples was carried out with the following conclusions.

1. The variance of welding pressure and welding duration within the boundary conditions concluded as the most influential control parameter on LSS of joints. According to the results, up to 7.67MPa joint strength was achieved.
2. Increasing levels of welding duration and amplitude resulted in higher energy consumption during welding. Moreover, structural degradation of composite was observed above a threshold energy value which also caused a sudden drop in LSS.
3. According to observations from fracture analysis, three different fracture modes namely interfacial seperation, nugget shear fracture and nugget pull-out fracture were observed from welded specimens.

# 6. CONCLUSION

The trend of using various high-performance TPCs instead of metallic parts has been popular due to enhanced mechanical properties. However, the mechanical performance of TPCs is mainly influenced by the type of reinforcement, continuity of reinforcement, type of the matrix, manufacturing methods, processing parameters and microstructure relations between the matrix and the reinforcement. Therefore, this thesis is motivated by aiming to fill the gap in the literature investigating the effects of processing parameters of a novel SCFR-ABS composite on the mechanical response with two different manufacturing methods named CM and USW. A two-stage experimental design approach was carried out during this research. According to the experimental&statistical results and microstructural analysis of fractured surfaces, research is concluded as follows.

The first stage of this study revealed that the tensile properties of SCFR-ABS composite are strictly affected by reinforcement content and molding temperature. Increasing the levels of two control parameters provided a basis for the tensile strength improvement up to around 85MPa. Furthermore, fiber inclusion into the system resulted in ductility decrease indicating brittle behavior of composite compared with the virgin polymer. However, it can be analyzed from the main effects plot for molding temperature that increasing this parameter shows a positive effect on tensile strain independent from the other parameters. Moreover, molding pressure had a limited impact on tensile properties. Therefore, carbon fiber content and molding temperature were found as the key processing parameters influencing tensile performance. On the other hand, the impact energy of composite relied mainly on molding pressure whose significance was found as over 50%. Surprisingly, analysis and experiments pointed out that reinforcement content has a limited effect of around 16% on the impact energy. Microstructural analysis of samples subjected to tensile and impact loadings revealed that fiber pull-out is the main fracture mechanism demonstrating weak interfacial adhesion between the fibers and the matrix. In addition, increasing molding temperature from level 1 to 3 provided a noticeable improvement on the tensile strength due to direct relationship between number of matrix pores and tensile properties.

The second stage of this study concentrated on achieving the maximum joint strength with the minimum welding energy in lap configuration. In the light of DOE conditions, welding pressure and time were concluded as the most outstanding control parameters affecting LSS of joints. It can be deduced from the main effects plot of welding pressure that shifting this parameter up led to a dramatic drop in LSS as the higher slopes indicate significance. Furthermore, up to 7.67MPa joint strength was achieved by applying Taguchi optimization. Besides, high levels of welding duration and amplitude consumed higher energy during welding due to the correlation between these parameters and welding energy. However, structural degradation of the composite which causes a sudden decrease in LSS was observed above a threshold energy value due to overheating and especially welding pressure increase. On the other hand, three different fracture modes categorized as interfacial separation, nugget shear fracture and nugget pull-out fracture were observed from the microstructure studies of welded specimens underlining the importance of processing parameters.

# FUTURE WORKS

This thesis provides preliminary knowledge about the mechanical and microstructural behavior of SCFR-ABS composite under different types of loadings with various manufacturing methods. In fact, this study can expand new horizons to fresh researches which can include the following suggestions listed below.

1. The number of level of processing parameters can be increased in order to better converge the optimum tensile strength, tensile strain and impact energy.
2. Tensile and impact samples can be manufactured with different fabrication techniques in order to compare the change in the mechanical response of composite.
3. LSS of joints can be improved via using flat EDs. Comparison of LSS with ED or without ED can be discussed.
4. LSS of joints can be discussed with another fusion bonding method for TPC which were mentioned Section 2.4.3.

# BIBLIOGRAPHY

[1] Yao SS, Jin FL, Rhee KY, Hui D, Park SJ. Recent advances in carbon-fiber-reinforced thermoplastic composites: A review. Composites Part B: Engineering 2018;142:241–50.

[2] Ishikawa T, Amaoka K, Masubuchi Y, Yamamoto T, Yamanaka A, Arai M, Takahashi J. Overview of automotive structural composites technology developments in Japan. Composites Science and Technology 2018;155:221–46.

[3] Fu SY, Lauke B, Mader E, Yue CY, Hu X. Tensile properties of short-glass-fiber and short-carbon-fiber-reinforced polypropylene composites. Composites Part A: Applied Science and Manufacturing 2000;31:1117-25

[4] Wan Y, Takahashi J. Tensile and compressive properties of chopped carbon fiber tapes reinforced thermoplastics with different fiber lengths and molding pressures. Composites Part A: Applied Science and Manufacturing 2016;87:271-81

[5] Song Y, Gandhi U, Sekito T, Vaidya UK, Vallury S, Yang A, Osswald T. CAE method for compression molding of carbon fiber reinforced thermoplastic composite using bulk materials. Composites Part A: Applied Science and Manufacturing 2018;114:388-97

[6] Goto K, Imai K, Arai M, Ishikawa T. Shear and tensile joint strengths of carbon fiber-reinforced thermoplastics using ultrasonic welding. Composites Part A: Applied Science and Manufacturing 2019;116:126–37.

[7] Palardy G, Shi H, Levy A, Le Corre S, Villegas IF. A study on amplitude transmission in ultrasonic welding of thermoplastic composites. Composites Part A: Applied Science and Manufacturing 2018;113:339-49.

[8] Tao W, Su X, Wang H, Zhang Z, Li H, Chen J. Influence mechanism of welding duration and energy director to the thermoplastic composite joints by ultrasonic welding. Journal of Manufacturing Processes 2019;37:196–202.

[9] Zhang Z, Wang X, Luo Y, Zhang Z, Wang L. Study on heating process of ultrasonic welding for thermoplastics. Journal of Thermoplastic Composite Materials 2010;23:647–64.

[10] Villegas IF. Strength development versus process data in ultrasonic welding of thermoplastic composites with flat energy directors and its application to the definition of optimum processing parameters. Composites Part A: Applied Science and Manufacturing 2014;65:27-37

[11] Crawford RJ. *Plastics Engineering*: General Properties of Plastics. Vol. 3rd ed. Amsterdam: Butterworth-Heinemann; 1998.

[12] Crompton TR. *Engineering Plastics*. Shrewsbury: Smithers Rapra; 2014.

[13] Engineering CoPS, Council N, Physical Sciences M, Staff DoEaP. *Polymer Science and Engineering: The Shifting Research Frontiers*. Washington, D.C.: National Academies Press; 1994.

[14] Ibeh CC. *Thermoplastic Materials: Properties, Manufacturing Methods, and Applications*. Baton Rouge: CRC Press LLC; 2011.

[15] Saldivar-Guerra E, Vivaldo-Lima E, Saldivar-Guerra E, Vivaldo-Lima E. *Handbook of Polymer Synthesis, Characterization, and Processing*. Somerset: John Wiley & Sons, Incorporated; 2013.

[16] Demaid A, Spedding V. *Classification of plastic materials.* Artifical Intelligence in Engineering 1996;10:9-20

[17] Mallick PK. *Materials, Design and Manufacturing for Lightweight Vehicles*. Cambridge: Elsevier Science & Technology; 2010.

[18] Goodman SH, Dodiuk H. *Handbook of Thermoset Plastics*. Burlington: Elsevier Science & Technology Books; 2013.

[19] Craver CD, Carraher CE. *Applied Polymer Science : 21st Century*. Oxford: Elsevier Science & Technology; 2000.

[20] Larson ER. *Thermoplastic Material Selection : A Practical Guide*. Bighamton: Elsevier Science & Technology Books; 2015.

[21] Barbero EJ. *Introduction to Composite Materials Design, Second Edition*. Bosa Roca: CRC Press LLC; 2010.

[22] Campbell F. *Structural Composite Materials*. Materials Park: A S M International; 2010.

[23] Bai J. *Advanced Fibre-Reinforced Polymer (FRP) Composites for Structural Applications: Advanced Fibre-Reinforced Polymer (Frp) Composites for Structural Applications*. Cambridge: Elsevier Science & Technology; 2013.

[24] Uddin N. *Developments in Fiber-Reinforced Polymer (FRP) Composites for Civil Engineering*. Cambridge, UK: Woodhead Publishing; 2013.

[25] Bajpai P. *Update on Carbon Fibre.* Shrewsbury: Smithers Rapra; 2013.

[26] Vaidya UK, Chawla KK. Processing of fibre reinforced thermoplastic composites. International Materials Reviews 2008;53(4):185-218.

[27] Offringa A, van Ingen JW, Buitenhuis A. Butt-joined, thermoplastic stiffened-skin concept development. SAMPE Journal 2012;48(2):7–15.

[28] Anandakumar P, Timmaraju MV, Velmurugan R. Development of efficient short/continuous fiber thermoplastic composite automobile suspension upper control arm. Materials Today:Proceedings 2020.

[29] Advani SG, Hsiao KT. *Manufacturing Techniques for Polymer Matrix Composites (PMCs)*. Cambridge: Elsevier Science & Technology; 2012.

[30] Elmarakbi A. *Advanced Composite Materials for Automotive Applications: Structural Integrity and Crashworthiness*. New York: John Wiley & Sons, Incorporated; 2013.

[31] Ozkoc G, Bayram G, Bayramli E. Effects of polyamide 6 incorporation to the short glass fiber reinforced ABS composites: an interfacial approach. Polymer 2004;45:8957-66.

[32] Lopes BJ, d'Almeida JRM. Initial development and characterization of carbon fiber reinforced ABS for future Additive Manufacturing applications. Materials Today: Proceedings 2019;8:719-30.

[33] Poli C. *Design for Manufacturing: A Structured Approach*. Burlington: Elsevier Science & Technology; 2001.

[34] Chanda M. *Plastics Technology Handbook*. Milton: CRC Press LLC; 2017.

[35] Dorworth LC, Gardiner GL, Mellema GM. *Essentials of Advanced Composite Fabrication & Repair*. Newcastle: Aviation Supplies and Academics, Inc.; 2015.

[36] Tekinalp HL, Kunc V, Velez-Garcia GM, Duty CE, Love LJ, Naskar AK, Blue CA, Ozcan S. Highly oriented carbon fiber–polymer composites via additive manufacturing. Composites Science and Technology 2014;105:144-50.

[37] Song Y, Gandhi U, Perez C, Osswald T, Vallury S, Yang A. Method to account for the fiber orientation of the initial charge on the fiber orientation of finished part in compression molding simulation. Composites Part A: Applied Science and Manufacturing 2017;100:244-54.

[38] Kauffer PH. *Injection Molding: Process, Design, and Applications*. Hauppauge: Nova Science Publishers, Incorporated; 2010.

[39] Kutz M. *Applied Plastics Engineering Handbook: Processing and Materials.* Binghamton: Elsevier Science & Technology Books; 2011.

[40] Fu SY, Mai YW, Lauke B, Xu G, Yue C-Y. Combined effect of fiber content and microstructure on the fracture toughness of SGF and SCF reinforced polypropylene composites. Journal of Materials Science 2002;37:3067-74.

[41] Cho J, Lee S-K, Eem S-H, Jang JG, Yang B. Enhanced mechanical and thermal properties of carbon fiber-reinforced thermoplastic polyketone composites. Composites Part A: Applied Science and Manufacturing 2019;126:105599.

[42] Li J, Cai CL. The carbon fiber surface treatment and addition of PA6 on tensile properties of ABS composites. Current Applied Physics 2011;11:50-54.

[43] Kuram E, Tasci E, Altan AI, Medar MM, Yilmaz F, Ozcelik B. Investigating the effects of recycling number and injection parameters on the mechanical properties of glass-fibre reinforced nylon 6 using Taguchi method. Materials and Design 2013;49:139-50.

[44] Karsli NG, Aytac A. Tensile and thermomechanical properties of short carbon fiber reinforced polyamide 6 composites. Composites Part B: Engineering 2013;51:270-75.

[45] Ozkan C, Karsli NG, Aytac A, Deniz V. Short carbon fiber reinforced polycarbonate composites: Effects of different sizing materials. Composites Part B: Engineering 2014;62:230-35.

[46] Molnar S, Rosenberger S, Gulyas J, Pukanszky B. Structure and impact resistance of short carbon fiber reinforced polyamide 6 composites. Journal of Macromolecular Science-Physics 1999; 38:721-35.

[47] Sato N, Kurauchi T, Sato S, Kamigaito O. Microfailure behaviour of randomly dispersed short fibre reinforced thermoplastic composites obtained by direct SEM observations. Journal of Materials Science 1991;26:3891-98.

[48] Zindani D, Kumar K. An insight into additive manufacturing of fiber reinforced polymer composite. International Journal of Lightweight Materials and Manufacture 2019;2:267-78.

[49] Love LJ, Kunc V, Rios O, Duty CE, Elliott AM, Post BK, Smith RJ, Blue CA. The importance of carbon fiber to polymer additive manufacturing. Journal of Materials Research Society 2014;29 (17):1893–98.

[50] Lay M, Thajudin NLN, Hamid ZAA, Rusli A, Abdullah MK, Shuib RK. Comparison of physical and mechanical properties of PLA, ABS and nylon 6 fabricated using fused deposition modeling and injection molding. Composites Part B: Engineering 2019;176:107341.

[51] Garzon-Hernandez S, Garcia-Gonzalez D, Jérusalem A, Arias A. Design of FDM 3D printed polymers: An experimental-modelling methodology for the prediction of mechanical properties. Materials and Design 2019;188:108414.

[52] Ngo TD, Kashani A, Imbalzano G, Nguyen KTQ, Hui D. Additive manufacturing (3D printing): A review of materials, methods, applications and challenges. Composites Part B: Engineering 2018;143:172-96.

[53] Moumen AE, Tarfaoui M, Lafdi K. Additive manufacturing of polymer composites: Processing and modeling approaches. Composites Part B: Engineering 2019;171:166-82.

[54] Ning FD, Cong W, Wei J, Wang S, Zhang M. *Additive manufacturing of CFRP composites using fused deposition modeling: Effects of carbon fiber content and length*. In: Proceedings of MSEC 2015, Charlotte, NC, USA, 2015.

[55] Zhang W, Cotton C, Sun J, Heider D, Gu B, Sun B, Chou TW. Interfacial bonding strength of short carbon fiber/acrylonitrile-butadienestyrene composites fabricated by fused deposition modeling. Composites Part B: Engineering 2018;137:51-59.

[56] Zhang W, Wu AS, Sun J, Quan Z, Gu B, Sun B, Cotton C, Heider D, Chou TW. Characterization of residual stress and deformation in additively manufactured ABS polymer and composite specimens. Composites Science and Technology 2017;150:102-10.

[57] Weng Z, Wang J, Senthil T, Wu L. Mechanical and thermal properties of ABS/montmorillonite nanocomposites for fused deposition modeling 3D printing. Materials and Design 2016;102:276-83.

[58] Yousefpour A, Hojjati M, Immarigeon JP. Fusion bonding-welding of thermoplastic composites. Journal of Thermoplastic Composite Materials 2004;17:303–41.

[59] Deng S, Djukic L, Paton R, Ye L. Thermoplastic–epoxy interactions and their potential applications in joining composite structures – A review. Composites Part A: Applied Science and Manufacturing 2015;68:121-32.

[60] Ageorges C, Ye L, Hou M. Advances in fusion bonding techniques for joining thermoplastic matrix composites: a review. Composites Part A: Applied Science and Manufacturing 2001;32:839-57.

[61] Meng L, Wan Y, Ohsawa I, Takahashi J. Effects of geometric parameters on the failure behavior of mechanically fastened chopped carbon fiber tape reinforced thermoplastics. Composites Structures 2019;229:111475.

[62] Pisano AA, Fuschi P. Mechanically fastened joints in composite laminates: Evaluation of load bearing capacity. Composites Part B: Engineering 2011;42:949-61.

[63] Pramanik A, Basak AK, Dong Y, Sarker PK, Uddin MS, Littlefair G, Dixit AR, Chattopadhyaya S. Joining of carbon fibre reinforced polymer (CFRP) composites and aluminium alloys – A review. Composites Part A: Applied Science and Manufacturing 2017;101:1-29.

[64] Thoppul SD, Finegan J, Gibson RF. Mechanics of mechanically fastened joints in polymer–matrix composite structures – A review. Composites Science and Technology 2009;69:301-29.

[65] Iqbal HMS, Bhowmik S, Benedictus R. Surface modification of high performance polymers by atmospheric pressure plasma and failure mechanism of adhesive bonded joints. International Journal of Adhesion & Adhesives 2010;30:418-24.

[66] Ebnesajjad S. *Handbook of Adhesives and Surface Preparation: Technology, Applications and Manufacturing*. Binghamton: Elsevier Science & Technology Books; 2010.

[67] da Costa AP, Botelho EC, Costa ML, Narita NE, Tarpani JR. A Review of Welding Technologies for Thermoplastic Composites in Aerospace Applications. Journal of Aerospace Technology and Management 2012;4:255-65.

[68] Stokes VK, Conway KR. A phenomenological study of the hot-tool welding of thermoplastics. 4. Weld strength data for several blends. Polymer 2001;42:7477-93.

[69] Balkan O, Demirer H, Yildirim H. Morphological and mechanical properties of hot gas welded PE, PP and PVC sheets. Journal of Achievements in Materials and Manufacturing Engineering 2008;31:60-70.

[70] Lagardere E, Lacrampe MF, Skawinski O, Krawczak P, Ducret C, Giletti M. A novel extrusion-welded sandwich structure for thermoplastic composite storage tanks. Sandwich Structures 7: Advancing with Sandwich Structures and Materials 2005;703-11.

[71] Amanat N, James NL, McKenzie DR. Welding methods for joining thermoplastic polymers for the hermetic enclosure of medical devices. Medical Engineering & Physics 2010;32:690-99.

[72] Pal K, Panwar V, Friedrich S, Gehde M. An Investigation on Vibration Welding of Amorphous and Semicrystalline Polymers. Materials and Manufacturing Processes 2016;31:372-78.

[73] Villegas IF, Bersee HEN. Ultrasonic Welding of Advanced Thermoplastic Composites: An Investigation on Energy-Directing Surfaces. Advances in Polymer Technology 2010;29:112-21.

[74] Paoletti A, Lambiase F, Di Ilio A. Optimization of friction stir welding of thermoplastics. Procedia CIRP 2015;33:562–7.

[75] Rezaee Hajideh M, Farahani M, Molla Ramezani N. Reinforced Dissimilar Friction Stir Weld of Polypropylene to Acrylonitrile Butadiene Styrene with Copper Nanopowder. Journal of Manufacturing Processes 2018;32:445–54.

[76] Banik N. A review on the use of thermoplastic composites and their effects in induction welding method. Materials Today Proceedings 2018;5:20239–49.

[77] Ahmed TJ, Stavrov D, Bersee HEN, Beukers A. Induction welding of thermoplastic composites-an overview. Composites Part A: Applied Science and Manufacturing 2006;37:1638–51.

[78] Stavrov D, Bersee HEN. Resistance welding of thermoplastic composites-an overview. Composites Part A: Applied Science and Manufacturing 2005;36:39–54.

[79] Brassard D, Dubé M, Tavares JR. Resistance welding of thermoplastic composites with a nanocomposite heating element. Composites Part B: Engineering 2019;165:779–84.

[80] Tutunjian S, Eroglu O, Dannemann M, Modler N, Fischer F. A numerical analysis of an energy directing method through friction heating during the ultrasonic welding of thermoplastic composites. Journal of Thermoplastic Composite Materials 2019:1–19.

[81] Troughton MJ. *Handbook of Plastics Joining : A Practical Guide*. Norwich, NY: William Andrew; 2008.

[82] Sancaktar E. Polymer adhesion by ultrasonic welding. Journal of Adhesion Science and Technology 1999;13:179–201.

[83] Palardy G, Villegas IF. Ultrasonic welding of thermoplastic composites with flat energy directors: Influence of the thickness of the energy director on the welding process. ICCM International Conference on Composite Materials 2015;2015-July:19–24.

[84] Villegas IF, Grande BV, Bersee HEN, Benedictus R. A comparative evaluation between flat and traditional energy directors for ultrasonic welding of CF/PPS thermoplastic composites. Composite Interfaces 2015;22:717–29.

[85] Villegas IF, Bersee HEN. Ultrasonic Welding of Advanced Thermoplastic Composites: An Investigation on Energy-Directing Surfaces. Advances in Polymer Technology 2010;29:112-21.

[86] Liu SJ, Chang IT. Optimizing the Weld Strength of Ultrasonically Welded Nylon Composites. Journal of Composites Materials 2002;36:611-24.

[87] Liu SJ, Chang IT. Factors Affecting the Joint Strength of Ultrasonically Welded Polypropylene Composites. Polymer Composites 2001;22:132-41.

[88] Wang K, Shriver D, Li Y, Banu M, Hu SJ, Xiao G, Arinez J, Fan HT. Characterization of weld attributes in ultrasonic welding of short carbon fiber reinforced thermoplastic composites. Journal of Manufacturing Processes 2017;29:124-32.

[89] ASTM D638, ASTM Standard test method for tensile properties of plastics, in D638-03. 2003. West Conshohocken (PA): ASTM International.

[90] D4812-19, Standard Test Method for Unnotched Cantilever Beam Impact Resistance of Plastics. West Conshohocken, PA; ASTM International, 2019.

[91] Oktem H, Erzurumlu T, Uzman I. Application of Taguchi optimization technique in determining plastic injection molding process parameters for a thin-shell part. Materials and Design 2007;28:1271-78.

[92] Huang CY, Wu CC. The EMI shielding effectiveness of PC/ABS/nickel-coated-carbon-

fibre composites. European Polymer Journal 2000;36:2729-37

[93] Huang CY, Pai JF. Optimum conditions of electroless nickel plating on carbon fibres for EMI shielding effectiveness of ENCF/ABS composites. European Polymer Journal 1998;34:261-67

[94] ASTM D3164, ASTM Standard test method for Strength Properties of Adhesively Bonded Plastic Lap-Shear Sandwich Joints in Shear by Tension Loading, in D638-03. 2003. West Conshohocken (PA): ASTM International.

[95] Villegas IF, Palardy G. Ultrasonic Welding of Thermoplastic Composite Coupons for Mechanical Characterization of Welded Joints through Single Lap Shear Testing. Journal of Visualized Experiments 2016;108, e53592.

[96] Savas LA, Tayfun U, Dogan M. The use of polyethylene copolymers as compatibilizers in carbon fiber reinforced high density polyethylene composites. Composites Part B: Engineering 2016;99:188–95.

[97] Fu SY, Lauke B. Fracture resistance of unfilled and calcite-particle-filled ABS composites reinforced by short glass fibers (SGF) under impact load. Composites Part A: Applied Science and Manufacturing 1998;29:631–41.

[98] Karsli NG, Aytac A. Effects of maleated polypropylene on the morphology, thermal and mechanical properties of short carbon fiber reinforced polypropylene composites. Materials and Design 2011;32:4069-73

[99] Karsli NG, Ozkan C, Aytac A, Deniz V. Characterization of poly(butylene terephthalate) composites prepared by using various types of sized carbon fibers. Materials and Design 2015;87:318-323

[100] Karsli NG, Ozkan C, Aytac A, Deniz V. Effects of sizing materials on the properties of carbon fiber-reinforced polyamide 6,6 composites. Polymer Composites 2013;34:1583-90.

[101] Patel N, Jain P. An investigation on mechanical properties in randomly oriented short natural fiber reinforced composites. Materials Today:Proceedings 2020.

[102] Zhao T, Palardy G, Villegas IF, Rans C, Martinez M, Benedictus R. Mechanical behaviour of thermoplastic composites spot-welded and mechanically fastened joints: A preliminary comparison. Composites Part B: Engineering 2017;112:224–34.

[103] Zhao T, Rans C, Villegas IF, Benedictus R. On sequential ultrasonic spot welding as an alternative to mechanical fastening in thermoplastic composite assemblies: A study on single-column multi-row single-lap shear joints. Composites Part A: Applied Science and Manufacturing 2019;120:1–11.

[104] Raza SF, Khan SA, Mughal MP. Optimizing the weld factors affecting ultrasonic welding of thermoplastics. The International Journal of Advanced Manufacturing Technology 2019;103:2053–67.

[105] Tiganis BE, Burn LS, Davis P, Hill AJ. Thermal degradation of acrylonitrile–butadiene–styrene (ABS) blends. Polymer Degradation and Stability 2002;76:425-434

[106] Wang K, Shriver D, Banu M, Jack Hu S, Xiao G, Arinez J, et al. Performance Prediction for Ultrasonic Spot Welds of Short Carbon Fiber-Reinforced Composites under Shear Loading. Journal of Manufacturing Science and Engineering Trans ASME 2017;139.

# VITA

The author was born on the 5th of January 1992, in Izmir, Turkey. He obtained his B.Sc. in Mechanical Engineering from Izmir Institute of Technology in 2015. After graduation, he started to work at MAT Filtration Systems located in Guzelbahce, Izmir in 2015 as a Mechanical Design Engineer and was responsible for the design&verification of pipelines of public aquarium filtration systems. After that, he shifted the working company and started to work at Vestel White Goods Inc., Dishwasher Factory, R&D Department as Mechanical Design Engineer in August 2016. Since 2017, he has worked both at the same company and pursued his M.Sc. degree in Mechanical Engineering at Ozyegin University. His research interests are mainly focused on the mechanical behavior of various unreinforced, reinforced polymers and their manufacturing&joining methods such as compression molding, injection molding, fused deposition modeling, ultrasonic welding and vibration welding.